ORGANOMETALLICS

pubs.acs.org/Organometallics Article

Disubstituted Ferrocenyl Iodo- and Chalcogenoalkynes as Chiral Halogen and Chalcogen Bond Donors

Victor Mamane,* Paola Peluso,* Emmanuel Aubert, Robin Weiss, Emmanuel Wenger, Sergio Cossu, and Patrick Pale

Cite This: https://dx.doi.org/10.1021/acs.organomet.0c00633 Read Online

ACCESS | Metrics & More | Article Recommendations | Supporting Information

ABSTRACT: Asymmetric catalysis based on halogen and chalcogen bonds (XB and ChB) is in its infancy, and the search for new chiral XB and ChB donors represents a crucial step toward its development. In this context, we designed and prepared new motifs containing three key substructures: namely, regions of electron charge density depletion centered on iodine and chalcogen atoms, the ethynyl functionality, and the planar chiral ferrocenyl platform. Nine ferrocenyl iodoalkynes were prepared as pure enantiomers by asymmetric synthesis. The XB donor property of racemic ferrocenyl iodoalkynes was demonstrated in solution in two benchmark reactions: the Ritter reaction and the benzoxazole synthesis from thioamides. In contrast, the ferrocenyl chalcogenoalkynes were far less active in these reactions. The potential of racemic and enantiopure ferrocenyl iodoalkynes as XB donors was also confirmed by X-ray diffraction analysis, showing I···C contacts between the electropositive σ hole of the iodine atom and electron-ich π clouds for all crystal structures studied in the solid state.

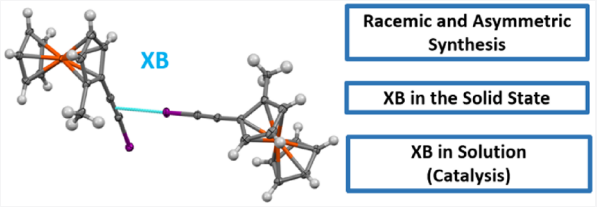

INTRODUCTION

In the past few years, halogen and chalcogen bonds (XB and ChB, respectively) have been recognized as important noncovalent interactions and rationalized through the so-called σ hole, which characterizes a covalently bonded atom of groups 13−18.[1] These atoms (σ-hole donors) bear a region with a positive electrostatic potential on unpopulated σ^* orbitals, allowing them to interact with a negative site (σ-hole acceptor: anion, lone electron pair, π electrons).

Applications based on XB and ChB have grown rapidly during the last 20 years, and important developments have emerged in crystal engineering, in biology, in supramolecular chemistry, and in catalysis.[2−8] However, the involvement of XB and ChB in stereoselective processes has remained unexplored until recently. We described XB- and ChB-driven HPLC enantioseparations of polyhalogenated 4,4′-bipyridines and related recognition mechanisms.[9−14] Beer's group described the enantioselective recognition of chiral anions of BINOL-based XB donors[15−18] and Kanger's group developed chiral triazole-based XB donors for the enantiodiscrimination of neutral acceptors.[19,20] In the field of catalysis, it is worth mentioning the works of Arai and co-workers, who obtained good enantiomeric excesses in asymmetric Mannich reactions between malononitrile and *N*-Boc imines or *N*-Boc α-ketimino esters using a quinidine-based chiral catalyst bearing a neutral XB donor functionality.[21,22] More recently, Huber and co-workers described the first example of asymmetric catalysis using a pure XB donor catalyst.[23] Despite these achievements, XB- and ChB-driven stereoselective processes and in particular asymmetric catalysis still remain huge challenges, as does the design of appropriate XB or ChB chiral donor molecules.[24]

In general, electron-withdrawing residues increase the σ holes of X and Ch atoms. In this regard, perfluorinated and cationic N-heterocyclic molecules are widely used for the synthesis of strong XB and ChB donors, which have found various applications to organocatalysis.[7,8] A different approach to increase σ holes is to attach the halogen atom, in particular iodine, to an acetylenic unit. Indeed, in these compounds, iodine is directly attached to a C_{sp} atom, where the contribution of the s orbital is higher in comparison to sp^2 and sp^3 carbons. Remarkably, iodoalkynes are good building blocks in crystal engineering[25−27] but they have been far less described in solution as XB donors. However, it has been known for a long time that iodoalkynes can form strong XB adducts in solution with Lewis bases, such adducts being observed by UV−vis[28] and by NMR.[29] Two recent examples highlighted the potential of these compounds in organic synthesis, the iodoalkyne behaving either as a catalyst[30] or as an activator.[31] The analogues thio- and selenoalkynes are known to be stable useful synthons in organic synthesis,[32−35] but the σ-hole donor properties of sulfur and selenium in these

Received: September 22, 2020

https://dx.doi.org/10.1021/acs.organomet.0c00633
Organometallics XXXX, XXX, XXX−XXX

derivatives have never been considered. It is thus worth exploring and possibly exploiting iodo- and more specifically thio- and selenoalkynes as XB or ChB (chiral) donors.

With the aim of developing new chiral XB and ChB donor molecules, we report herein the synthesis of chiral ferrocenyl iodo- and chalcogenoalkynes by combining the σ-hole donor properties of iodine, sulfur, and selenium when they are bonded to an alkyne and the planar chirality of ferrocene.[36] As the ferrocene substitution pattern might influence iodine polarizability, both 1,2- and 1,3-disubstituted chiral ferrocene derivatives were considered in this work. In comparison to 1,2-disubstituted ferrocenes, whose applications are numerous,[37,38] the 1,3-disubstituted ferrocenes have been much less described in the literature. A few derivatives have been reported with interesting activity in catalysis,[39] medicinal chemistry,[40] and supramolecular chemistry, serving as hydrogen-bond[41] or XB[42] receptors.

The σ-hole donor property of the selected compounds was investigated in solution by a preliminary evaluation of their performance in the Ritter reaction[43] and in the benzoxazole synthesis from thioamides.[30] The potential of racemic and enantiopure ferrocenyl iodoalkynes as XB donors was also evaluated in the solid state by X-ray diffraction (XRD) analysis.

RESULTS AND DISCUSSION

Design and Electrostatic Potential Analysis. The design of the compounds reported here was based on 1,2- or 1,3-disubstituted ferrocenes, in which one of the substituents is the iodo-, thio- and selenoethynyl moiety carrying σ holes and the other is an electron-withdrawing group in order to increase the adjacent σ-hole depth. This design was also substantiated by calculating the electrostatic potential (V) on focused regions of these molecules, so that local electron charge density, especially of σ-hole regions, could be anticipated.

A general strategy was thus designed for the synthesis of various ferrocenyl-based iodoalkynes **9**−**13** and chalcogenoalkynes **16** and **17** starting from 1,2- or 1,3-disubstituted ferrocenes **1** and **2** (Scheme 1). The σ-hole donor atom (I, S, or Se) would be introduced in the late stage from silyl-protected alkynes **4**, **5**, and **6**−**8** through a deprotection−functionalization sequence that can be conducted in one or two steps. With bromo-substituted ferrocenyl compounds **4a** and **5a** (X = Br) as the starting materials, the introduction of aryl and methyl groups can be carried out through Suzuki coupling or bromine/lithium exchange followed by electrophilic quenching. The alkyne function in derivatives **4**−**8** can be introduced by using a selective Sonogashira coupling with the readily available iodoferrocenyl derivatives **1** and **2**.

Scheme 1. General Strategy for the Synthesis of Ferrocenyl-Based Iodoalkynes 9−13 and Chalcogenoalkynes 16 and 17

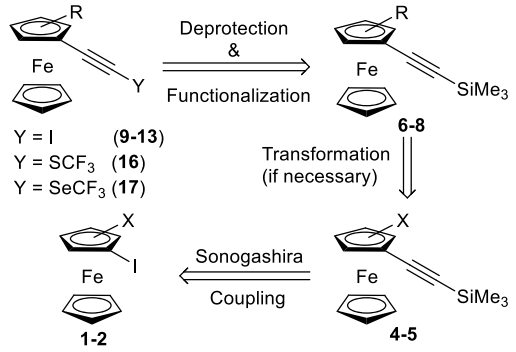

In the framework of a rational design approach, the V values of iodo-, thio- and selenoethynylferrocenes **9a**−**c**, **10b**, **16a**, and **17a** were computed on a 0.002 au molecular isosurface (V_S).

The V_S values of pentafluorobenzenes **18**−**20**, halobenzenes **21**-**23** and **25**−**30**, and haloferrocenes **1b** and **3a**−**b**, as well as nonsubstituted iodoethynylbenzene **24** and iodoethynylferrocene **31**, were computed as benchmarks in order to evaluate the effect of both the ferrocenyl and ethynyl substructures on the local electron charge density of the σ-hole regions. For this purpose, the V_S maxima ($V_{S,max}$) on the σ holes centered on I and Ch (S, Se) atoms were compared (Table 1) in order to explore the effect of subtle structure modifications on the σ-hole depth.

The geometry of all compounds given in Table 1 was optimized using density functional theory with the B3LYP functional (completed with D3 dispersion corrections) and the Def2TZVPP basis set. The local maxima of the electrostatic potential ($V_{S,max}$) values were calculated on the 0.002 au isodensity surface (see the Supporting Information for details).

As expected, these theoretical results confirmed the beneficial effect of the alkyne moiety on the iodine σ-hole depth (Table 1, entry 4 vs entries 12 and 7 vs entry 19). The results also showed that the activation ability of the alkyne function toward the iodine σ hole is comparable to and even slightly better than the effect of perfluorination (entry 10 vs entry 1). This effect can be increased by an additional electron-withdrawing halogen atom (entry 10 vs entries 11−13 and 16). It is worth noting that the obtained $V_{S,max}$ values for the series **24**−**27** and **30** are in good agreement with the donor/acceptor nature of substituents in other reports concerning similar iodoalkyne-based structures.[27,44−46] Interestingly, when the chlorine was placed in the 3-position, the iodine σ hole increased (entry 12 vs entry 16). The beneficial effects on the iodine σ hole due to the additional halogen atom (entry 17 vs entries 18−20) and its position (entry 19 vs entry 23) are also observed in the ferrocenyl iodoalkyne series. However, lower $V_{S,max}$ values are always obtained for the ferrocenyl derivatives in comparison to the phenyl derivatives (entries 10−13 vs entries 17−20 and entry 16 vs entry 23), confirming the greater electron-donating ability of ferrocene in comparison to phenyl. Nevertheless, the $V_{S,max}$ values of ferrocenyl compounds **9a**−**c** and **10b** are still comparable to that of iodopentafluorobenzene **18** (entry 1 vs entryies18−20); therefore, interesting σ-hole-based properties can be expected with these compounds.

Regarding the chalcogen atoms, they possess two σ holes, one on the elongation of the C_{CF3}−Ch bond and one on the elongation of the $C_{Ar/Fc}$−Ch or $C_{ethynyl}$−Ch bond. As a matter of fact, in nonsymmetrical compounds such as **22**, **23**, **3a**,**b**, **28**, **29**, **16a**, and **17a**, two conformations are observed depending on the position of the CF_3 group with respect to the chlorine atom. Interestingly, in compounds **22**, **23**, and **3a**−**b** (Table 1, entries 5, 6, 8, and 9), the $V_{S,max}$ values along the C_{CF3}−Ch bond for the two conformers are completely different and in three cases the σ hole of one of the two conformers cannot be observed (entries 5, 8, and 9). This effect is due to the contribution of neighboring atoms to the analyzed molecular surface. For example, in the second conformation of compound **23**, the expected selenium σ hole opposite to the CF_3−Se bond is directly oriented toward the negative crown of

https://dx.doi.org/10.1021/acs.organomet.0c00633
Organometallics XXXX, XXX, XXX−XXX

Table 1. $V_{S,max}$ (kJ/mol) Values Calculated on I and Ch σ-Holes (B3LYP-D3/Def2TZVPP)[a]

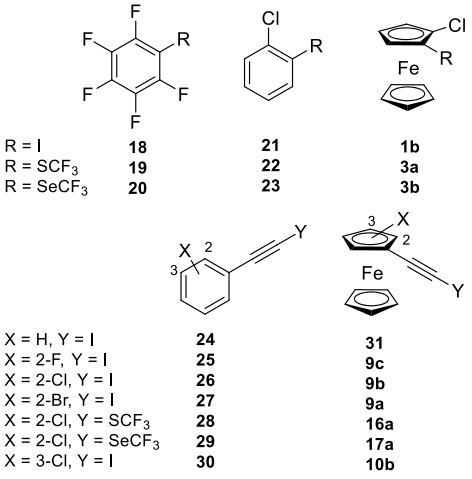

		$V_{S,max}$ (kJ/mol)[a]			
entry	compound	I	Ch ($C_{Ar/Fc}$–Ch)[b]	Ch ($C_{ethynyl}$–Ch)[b]	Ch (C_{CF3}–Ch)[b]
1	**18**	181			
2	**19**		100		140
3	**20**		136		158
4	**21**	122			
5[c]	**22**		54/56		94/-
6[c]	**23**		87/87		113/33
7	**1b**	119			
8[c]	**3a**		47/51		-/81
9[c]	**3b**		81/86		-/101
10	**24**	183			
11	**25**	187			
12	**26**	188			
13	**27**	189			
14[c]	**28**			95/95	97/106
15[c]	**29**			138/135	124/131
16	**30**	194			
17	**31**	176			
18	**9c**	182			
19	**9b**	182			
20	**9a**	182			
21[c]	**16a**			78/83	91/84
22[c]	**17a**			119/124	115/110
23	**10b**	185			

[a]Calculations were performed by using the Gaussian09 Version D.01 program (see the Supporting Information for details). [b]Corresponds to the hole along the C_I–Ch axis. [c]Two conformations were observed for these compounds.

the adjacent chlorine atom, leading to a V_S value smaller than that in the first conformation, where the same σ hole points toward the exterior of the molecule. In the case of **3b** this effect is even more pronounced, since the expected σ hole points toward a hydrogen atom of the neighboring cyclopentadienyl ring and appears buried inside the chosen molecular envelope and is thus not revealed on this surface (see Figure S26 in the Supporting Information).

From the results, it can also be noted that the alkyne function also polarizes sulfur and selenium atoms, increasing the σ-hole depth in both the phenyl (Table 1; for S, entry 5 vs entry 14 and for Se, entry 6 vs entry 15) and ferrocenyl (for S, entry 8 vs entry 21, and for Se, entry 9 vs entry 22) series. The calculations also confirmed the effect of shifting from sulfur to selenium in all of the chalcogen series, for which the σ hole depth always increases.

On the basis of V_S analysis, the alkyne substructure proved to be a powerful tool to polarize both iodine and chalcogens, generating σ-hole regions potentially able to promote the catalytic activity of ferrocenyl derivatives **9**–**13**, **16**, and **17**.

Racemic synthesis. The starting substituted iodoferrocenes **1a**–**d** and **2a**–**c** have been described in the literature and were prepared accordingly (Scheme 2).[47−49]

Scheme 2. Starting Substituted Iodoferrocenes

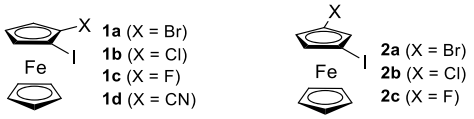

The ethynyl moiety was then introduced on 1,2- and 1,3-iodoferrocenes **1** and **2** by Sonogashira coupling with trimethylsilylacetylene. Classical conditions, based on $PdCl_2(PPh_3)_2$ and CuI as catalysts and on diisopropylamine as base and solvent,[50] provided variable results depending on the X substituent nature (Scheme 3, conditions A).

Scheme 3. Sonagashira Coupling of Iodoferrocenes 1 and 2

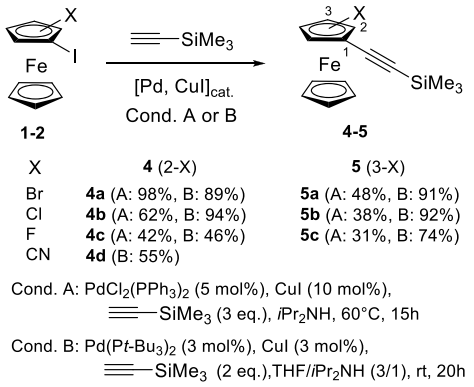

An optimization study performed on 1-bromo-2-iodoferrocene (**1a**) revealed that 3 equiv of trimethylsilylacetylene was necessary to achieve complete conversion. The expected compound **4a** was thus isolated with 98% yield. However, the yield dropped significantly as the electron-withdrawing ability of the atom adjacent to iodine increased and when the substituent was placed in the 3-position to iodine. Along with the expected compounds **4b**,**c** or **5a**–**c**, a substantial amount of the deiodinated starting material was isolated. In the case of **4d**, the so-formed cyanoferrocene could not be removed by chromatography (see Scheme S1 in the Supporting Information for more details).

The hydrodehalogenation reaction could be completely suppressed by using $Pd(P\text{-}t\text{-}Bu_3)_2$, previously described as a highly active catalyst in the Sonogashira reaction of 1,1′-diiodoferrocene.[51] Except for **4c**, yields were significantly improved and compound **4d** could be obtained in pure form after the unreacted starting material was removed (Scheme 3, conditions B).

To compare with the effect of the halogeno or cyano substituents, neutral non-electron-withdrawing groups were also introduced on the ferrocenyl unit. The simple methyl

https://dx.doi.org/10.1021/acs.organomet.0c00633
Organometallics XXXX, XXX, XXX−XXX

group was selected, as well as two aryl groups, phenyl and the larger 2-naphthyl (Scheme 4). The introduction of the latter was readily achieved through a Suzuki reaction.

Scheme 4. Arylation and Methylation of Bromoferrocenylacetylenes 4a and 5a

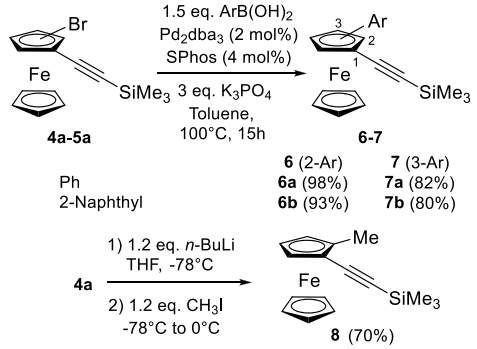

Coupling phenyl- and 2-naphthylboronic acids with bromo-substituted ferrocenylalkynes **4a** and **5a** was efficiently performed by using 2-dicyclohexylphosphino-2′,6′-dimethoxybiphenyl (SPhos) as a ligand and potassium phosphate as a base in toluene at 100 °C.[52] Indeed, good yields ranging from 80% to 98% were obtained for derivatives **6** and **7**. The methyl group was introduced by addition of *n*-BuLi on compound **4a** followed by quenching the lithiated ferrocenyl species. Derivative **8** was thus obtained with a good yield of 70% (Scheme 4).

For the synthesis of ferrocenyl iodoalkynes **9**−**13**, we explored the possibility to perform in one step the trimethylsilyl (TMS) group removal and the iodination of compounds **4**−**8**.

The combination of silver(I) fluoride and *N*-iodosuccinimide (NIS) has already been described for this purpose with a variety of TMS-protected alkynes.[53] Although the expected iodoalkynes were obtained in all cases, the yields were generally low to moderate (Scheme 5, conditions a). This could be due to oxidation of the ferrocene moiety by the silver salts present in the reaction mixture.[54,55]

With the aim of avoiding silver salts and of increasing the yields, a two-step procedure was tested. TMS-alkynes **4b** and **5b** were first deprotected with KOH in methanol at room temperature to give alkynes **14** and **15** with good yields (Scheme 5, conditions b). These alkynes were then treated again with KOH before addition of NIS[56] to give iodoalkynes **9b** and **10b** with good yields (Scheme 5, conditions c). Since KOH is used in the two steps, a one-pot procedure was employed with **4b** and **5b**, directly furnishing iodoalkynes **9b** and **10b** with yields superior to those of the two-step procedure. This protocol was therefore applied to TMS-alkynes **4a,c,d** and **5c**, greatly increasing the yields of the corresponding iodoalkynes **9a,c,d** and **10c** (Scheme 5, d).

For the synthesis of chalcogenoalkynes **16** and **17**, 2- and 3-chloroferrocenyl acetylenes **14** and **15** were functionalized through lithiation and electrophilic quenching with donors of SCF_3 and $SeCF_3$ groups. Alkyne deprotonation of **14** and **15** was performed with *n*-BuLi, and the resulting lithioalkynes were trapped with *N*-methyl-*N*-(trifluoromethylsulfanyl)-aniline[57] to give thioalkynes **16a,b** and with the *in situ* generated $ClSeCF_3$[58] to furnish selenoalkynes **17a,b**. Unexpectedly, **17b** was obtained as an inseparable mixture with

Scheme 5. Preparation of Ferrocenyliodoalkynes 9-13 through Deprotection−Iodination of Compounds 4−8[a]

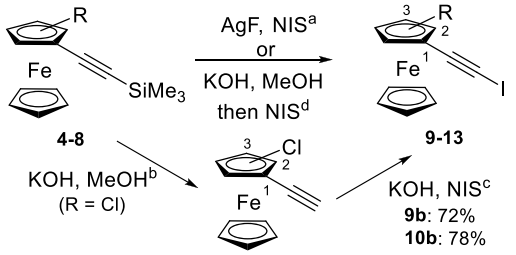

R	2-R	3-R
Br	**9a** (a: 56%, d: 71%)	**10a** (a: 84%)
Cl	**9b** (a: 48%, d: 77%)	**10b** (a: 50%, d: 80%)
F	**9c** (a: 42%, d: 93%)	**10c** (a: 36%, d: 80%)
CN	**9d** (d: 85%)	
Ph	**11a** (a: 72%)	**12a** (a: 45%)
2-Naphthyl	**11b** (a: 63%)	**12b** (a: 44%)
CH_3	**13** (a: 50%)	

Conditions:

[a] 1.05 eq. AgF, 1.05 eq. NIS, CH_3CN, rt, 15h
[b] 2.5 eq. KOH, MeOH, rt, 2h
[c] 2.5 eq. KOH, 1.5 eq. NIS, MeOH, rt, 2h
[d] 1) 5 eq. KOH, MeOH, rt, 2h; 2) 1.5 eq. NIS, rt, 2h

[a]Conditions: (a) 1.05 equiv of AgF, 1.05 equiv of NIS, CH_3CN, rt, 15 h; (b) 2.5 equiv of KOH, MeOH, rt, 2 h; (c) 2.5 equiv of KOH, 1.5 equiv of NIS, MeOH, rt, 2 h; (d) (1) 5 equiv of KOH, MeOH, rt, 2 h, (2) 1.5 equiv of NIS, rt, 2 h.

chloroalkene **18**.[59] Therefore, the **17b**/**18** mixture was treated with an excess of LiOH in DMSO[60] to deliver the pure compound **17b** with a moderate overall yield (Scheme 6).

Evaluation of Ferrocenyl Iodo- or Chalcogenoalkynes: C−Br and Thioamide Activation. In order to evaluate the σ-hole donor properties in solution of the new ferrocene-based iodo- and chalcogenoalkynes, we have

Scheme 6. Synthesis of Ferrocenyl-Based Thioalkynes 16a,b and Selenoalkynes 17a,b

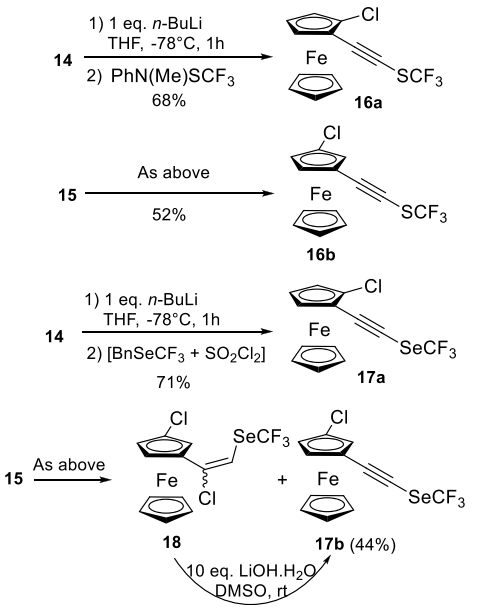

https://dx.doi.org/10.1021/acs.organomet.0c00633
Organometallics XXXX, XXX, XXX−XXX

considered two benchmark reactions: the Ritter reaction,[61] allowing the transformation of benzhydryl bromide **32** to acetamide **33**, and the synthesis of benzoxazole **36** from thioamide **34**[62] (Scheme 7). In order to study the influence of

Scheme 7. XB or ChB Activation of C−Br and Thioamide

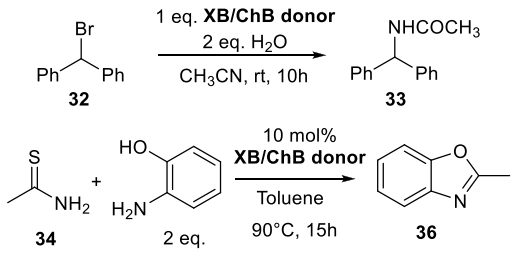

the substituent in both reactions, five compounds of the 2-substituted ferrocenyl iodoalkyne family (**9a−c** and **11a,b**) were tested. Moreover, the effects of the substituent position and the nature of the donor atom were also evaluated by using compounds **10b** and **17a** (Table 2).

Table 2. Results of Ritter Reaction and Benzoxazole Synthesis

			yield (%)	
XB/ChB donor	X/Ch	R	**33**[a]	**36**[c]
9a	I	2-Br	100	72
9b	I	2-Cl	91	86
10b	I	3-Cl	94	64
9c	I	2-F	35	86
11a	I	2-Ph	100	97
11b	I	2-Naph	100	83
17a	Se	2-Cl	35[b]	<5%

[a]^{1}H NMR conversions obtained by integration of peaks at 6.44 ppm (starting material) and at 5.77 ppm (product) in CD_3CN.[31] [b]60% conversion after 24 h. [c]^{1}H NMR yields by using DMF as an internal standard.[30]

Ritter-type reactions[63] involve the nucleophilic substitution of an alcohol, sulfate, or halide group by acetonitrile or related nitriles, usually used as the solvent. The resulting nitrilium is then hydrolyzed to the corresponding amide by added water. Depending on the leaving group nature, electrophilic assistance could facilitate the reaction and catalysis could be established. Lewis acids could act as such, and some could catalyze such reactions.[64] With σ-hole-based organocatalysts and halogenated substrates, the Ritter reaction is not catalytic due to its mechanism, close to an S_N1 process. In this reaction, the σ-hole donor interacts with the bromine of the substrate (compound **32** here; Scheme 7) to abstract it and the nucleophilic acetonitrile solvent replaces it. Nevertheless, the Ritter reaction allows a reliable evaluation of the σ-hole donor ability in solution.[31,43,65,66] All of the ferrocenyl derivatives examined were able to efficiently promote the expected transformation, except for fluoro derivatives (Table 2).

In the 2-haloferrocenyl iodoalkyne series **9a−c**, high conversions were obtained with the 2-bromo and 2-chloro derivatives **9a,b**, whereas a low conversion of 34% was observed with the 2-fluoro derivative **9c**. This difference in reactivity was unexpected with regard to the calculated $V_{S,max}$ values (Table 1, entries 18−20). A comparison of the 2- and 3-chloro derivatives **9b**/**10b** showed that the position of the halogen on the ferrocene moiety has very little effect on the reactivity but is in agreement with their slightly different $V_{S,max}$ values (Table 1, entry 23 vs entry 19). Surprisingly, the 2-arylferrocenyl iodoalkynes **11a,b** were as effective as the 2-bromo derivative **9a** but were more effective than the 2-chloro analogue **9b**, despite the stronger electron-withdrawing character of the latter.

These results revealed that the iodine σ hole is well activated by the alkyne function and that the substituent on the ferrocene moiety only has a moderate influence on reactivity, except for the strongly electron withdrawing fluoride. In contrast, the nature of the σ-hole donor has a strong influence on the reaction efficiency. Indeed, with the seleno derivative **17a**, the reaction proved to be slower, giving only 35% conversion after 10 h and 60% conversion after 24 h.

Benzoxazoles are important compounds due to their various biological activities and their roles in fluorescent and/or electroluminescent materials.[67] In 2016, Matsuzawa and co-workers have shown that iodoalkynes are able to catalyze the synthesis of benzoxazole from thioamides and 2-aminophenol on the basis of an iodine−sulfur interaction.[30] This reaction is thus worthy of comparison (Table 2). Interestingly, all of the ferrocenyl iodoalkynes were able to act as a catalyst and gave the expected benzoxazole **36**. High yields were obtained with the 2-chlorinated and 2-fluorinated compounds **9b,c**, whereas a lower yield was obtained with the 2-brominated analogue **9a**. In contrast to the Ritter results, the 3-chloro catalyst **10b** proved to be less effective, as the yield significantly dropped (64 vs 86%). For the Ritter reaction, the aryl-substituted ferrocenyl iodoalkynes **11a,b** were very efficient, giving high to quantitative yields of benzoxazole **36**. The selenium derivative **17a** proved again to be less efficient than the iodinated derivatives, since almost no benzoxazole was formed during the reaction.

In summary, with regard to the results of Table 2, the effects of nature and position of the halogen substituent on the activity of the iodoalkynes as activators or catalysts in the considered reactions are very difficult to analyze. It is clear, however, that the aryl-substituted compounds **11a,b** are very active in both reactions, which opens up the possibility to use them or other analogous substituents in asymmetric catalysis.

Asymmetric Synthesis of Ferrocenyl Iodoalkynes. Considering the above results, we decided to focus only on the synthesis of enantiopure ferrocenyl iodoalkynes. As shown through the racemic synthesis, compounds **4a** and **5a** are key intermediates for the synthesis of ferrocenyl iodoalkynes bearing substituents of different natures. For the 1,2-disubstituted series, we considered the preparation of enantiopure (S_{Fc})-**1a** as described in the literature,[68] but the yields and the enantiomeric excess that we obtained were unsatisfactory. Another useful enantiopure 1,2-substituted ferrocenyl synthon, the (S_s,S_{Fc})-sulfinylferrocenylboronic acid, attracted our attention, but it is suitable only for the preparation of aryl-substituted ferrocenes.[69]

We finally turned our attention to Kagan's method, which delivers enantiopure 2-substituted ferrocenecarboxaldehydes.[70] In particular, 2-bromoferrocenecarboxaldehyde ((S_{Fc})-**36**) was prepared[71] and transformed to the alkyne (S_{Fc})-**37** through a Seyferth−Gilbert homologation with Ohira−Bestmann reagent **38**.[72] A TMS group was then introduced on the alkyne to give the key compound (S_{Fc})-**4a**. With regard to the 1,3-disubstituted series, enantiopure compound **5a** was not available but the iodinated analogue (S_{Fc})-**39** has been

https://dx.doi.org/10.1021/acs.organomet.0c00633
Organometallics XXXX, XXX, XXX−XXX

described in the literature.[73] It was then transformed to the key compound (S_{Fc})-**41** through alkyne (S_{Fc})-**40** (Scheme 8).

Scheme 8. Synthesis of Enantiopure Key Compounds (S_{Fc})-4a and (S_{Fc})-41

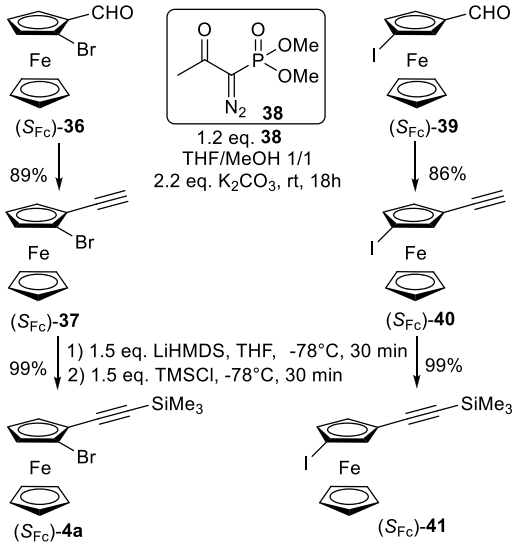

On one hand, when the experimental conditions set up for the Suzuki coupling of related compounds were applied (see Scheme 4), compounds (S_{Fc})-**4a** and (S_{Fc})-**41** were very efficiently transformed to (S_{Fc})-**6a,b** and (S_{Fc})-**7a,b**, respectively (Scheme 9, left). On the other hand, halogen−lithium

Scheme 9. Functionalization of (S_{Fc})-4a and (S_{Fc})-41

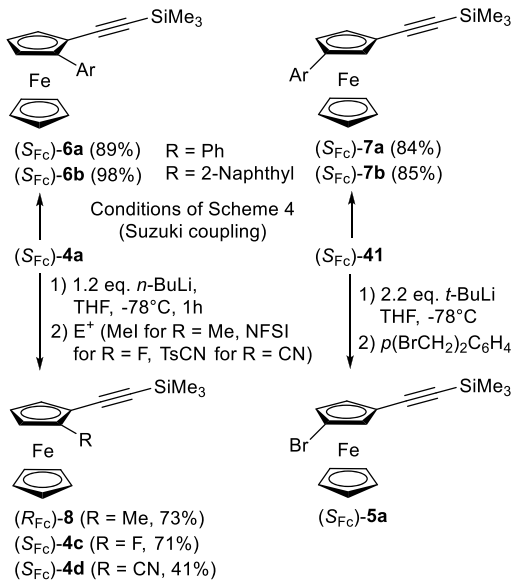

exchange followed by electrophilic quenching afforded differently substituted derivatives. With (S_{Fc})-**4a** as the starting material, quenching the lithiated species with MeI, *N*-fluorobenzenesulfonimide (NFSI), and *p*-toluenesulfonyl cyanide (TsCN) delivered compounds (R_{Fc})-**8**, (S_{Fc})-**4c**, and (S_{Fc})-**4d**, respectively. Addition of α,α'-dibromoxylene to the lithiated intermediate obtained from (S_{Fc})-**41** furnished (S_{Fc})-**5a**, which contained small amounts of inseparable impurities (Scheme 9, right).

Finally, the deprotection−iodination methods (see Scheme 5) were applied to all enantiopure/enantioenriched ferrocenyl trimethylsilylethynes. This sequence furnished diversely substituted ferrocene iodoethynes: i.e., (S_{Fc})-**9a,c,d**, (S_{Fc})-**10a**, (S_{Fc})-**11a,b**, (S_{Fc})-**12a,b**, and (R_{Fc})-**13** (Scheme 10).

Scheme 10. Synthesis of Enantiopure Ferrocenyliodoalkynes

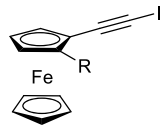

(S_{Fc})-**9a** (R = Br, 98.3% ee). Cond. a: 53%; Cond. d: 87%
(S_{Fc})-**9c** (R = F, 92.8% ee). Cond. a: 51%
(S_{Fc})-**9d** (R = CN, 98.7% ee). Cond. a: 77%
(S_{Fc})-**11a** (R= Ph, 96.8% ee). Cond a.: 59%
(S_{Fc})-**11b** (R = 2-Naph, 97.4% ee). Cond. a: 67%
(R_{Fc})-**13** (R = Me, 97.3% ee). Cond. a: 39%; Cond. d: 73%

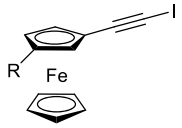

(S_{Fc})-**10a** (R = Br, 93.7% ee). Cond. a: 38% (after 2 steps)
(S_{Fc})-**12a** (R = Ph, 99.9% ee). Cond. a: 56%
(S_{Fc})-**12b** (R = 2-Naph, 99.9% ee). Cond. a: 49%;
Cond. d: 62%

The enantiomeric purity of compounds (S_{Fc})-**9a,c,d**, (S_{Fc})-**10a**, (S_{Fc})-**11a,b**, (S_{Fc})-**12a,b**, and (R_{Fc})-**13** was determined through high-performance liquid chromatography (HPLC) on polysaccharide-based chiral columns. For compounds **9a,d**, **10a**, **11b**, **12a,b**, and **13**, the proper combination of column and mobile phase was optimized, allowing us to obtain baseline enantioseparations. For compounds **9c** and **11a** only partial separation was achievable. For all compounds, enantiomeric excesses of ≥92.8% were measured (Scheme 10; see see Table S1 and Figure S1−S9 in the Supporting Information for details).

Solid-State Analysis. With these racemic and chiral ferrocenyl iodoethynes in hand, their σ-hole donor properties in the solid state were investigated by X-ray diffraction analysis (XRD) when possible. Crystal structures were determined by single-crystal XRD for a selected number of compounds. Hirshfeld molecular surfaces were computed for these structures (except for **9c**, which presents a disorder linked to symmetry), and actual surface contacts were compared to equiprobable contacts in order to derive the enrichment ratios (E).[74] As seen in Table S2) in the Supporting Information, Fe atoms in these ferrocenyl compounds are almost fully buried between the cyclopentadienyl rings, offering a very small contribution to the total molecular surface; thus, variations of this small surface between actual and equiprobable contacts are meaningless and will not be discussed. An enrichment ratio E larger (respectively smaller) than 1 means that the considered contact is enriched (respectively impoverished) in the actual crystal structure in comparison to the situation of equiprobable contacts. It can be noted (Tables S3−S10) that, despite the richness of aromatic groups in the studied compounds, no $\pi\cdots\pi$ interaction is observed, carbon···carbon contacts being clearly under-represented (E(C···C) = 0.7−0.8), except for (S_{Fc})-**12a**, in which the phenyl groups stack in somewhat long $\pi\cdots\pi$ contacts (E(C···C) = 1.06; intercentroid distance of 4.187 Å;

https://dx.doi.org/10.1021/acs.organomet.0c00633
Organometallics XXXX, XXX, XXX−XXX

tilt angle of 23.96°). Whereas H···H contacts are under-represented as well, contacts of hydrogen atoms with carbon and iodine atoms are over-represented (except in **13** with E(H···I) = 0.97).

In all obtained crystal structures, I···C XBs are observed between the electropositive σ hole of the iodine atom and electron-rich π clouds (Tables S3−S10 and Table S11). Interestingly, the XB acceptors vary and can be the alkyne carbon atoms[75] ((S_{Fc})-**12a**, (R_{Fc})-**13**, (S_{Fc})-**9a**), the cyclopentadienyl rings bearing the alkyne group (**13**, (S_{Fc})-**11a**, (S_{Fc})-**11b**), the unsubstituted cyclopentadienyl rings[76] (**9c**, (S_{Fc})-**9c**), or the naphthyl group (**11b**). The negatively charged belts usually found around polarized heavy halogen atoms (see the Supporting Information) are not involved as σ-hole acceptors in these structures; thus, no halogen···halogen bonds are evidenced for these compounds. Indeed, as can be seen for example in Figure S29 (compound **9b**) the ethynyl group offers a more negative V_S value in comparison to the bonded iodine atom itself.

These halogen interactions form infinite corrugated molecular chains in most of the structures (**9c**, **11b**, (R_{Fc})-**13**, (S_{Fc})-**9a**, (S_{Fc})-**9c**, (S_{Fc})-**11a**, (S_{Fc})-**11b**, (S_{Fc})-**12a**) (Figure 1 and Figures S10−S15). These chains stack to form planes

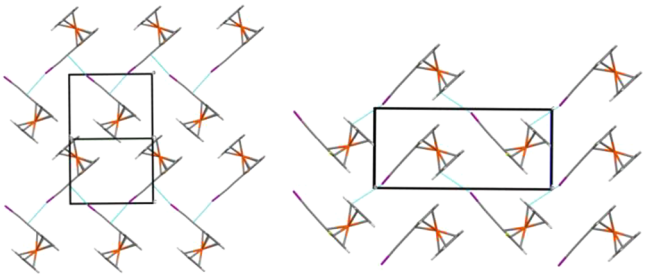

Figure 1. Planes containing the stacking of chains made of I···C halogen bonds (highlighted in cyan) in (S_{Fc})-**9a** (left, (101) plane) and in (S_{Fc})-**9c** (right, (010) plane).

which then interact through numerous H···C contacts to form 3D structures. Further H···F and π···π contacts can be noticed, respectively, in (S_{Fc})-**9c** and **9c**, and in (S_{Fc})-**12a** (see the Supporting Information).

One can distinguish two types of such planes among the structures, which can be grouped into two families. In the first family the infinite chains are relatively separated ((S_{Fc})-**9a**, (R_{Fc})-**13**, associated with a relatively large in-plane area per molecule), but in the second family these chains are more intimately nested and these structures have a relative small in-plane area per molecule ((S_{Fc})-**11a**, (S_{Fc})-**11b**, **11b**, (S_{Fc})-**12a**, (S_{Fc})-**9c**, **9c**) (Table S11).

The thickness of the planes depends on the R substituent adjacent to the iodoalkyne functionality (Figure S16), and the thinner is obtained for the smallest R group (**9c** and (S_{Fc})-**9c** where R = F). The thickness also depends on the molecular orientation relative to the plane, with for example (S_{Fc})-**11b** and **11b** where R = naphthyl exhibiting ∼30% plane width difference (Table S11).

The two members of the first family are isostructural ((R_{Fc})-**13** and (S_{Fc})-**9a**), differing only in Me/Br substitution. In the second family, the structures offer different levels of similarities. (S_{Fc})-**11a** and (S_{Fc})-**11b** both crystallize in $P2_12_12_1$ space group with similar a and b unit cell parameters; these two structures are not strictly isostructural but nevertheless share common packing characteristics, both having very similar (001) molecular packing planes (Figures S10, S11, and S17) formed by the stacking of the infinite I···C XB chains (Table S11). The main difference between the crystal structures of these two compounds is then the packing of their (001) planes along the [001] direction, where one of the two structures can be deduced from the other by a translation of half the b unit cell parameter. The larger difference in c unit cell parameters arises from the fact that the aromatic rings are oriented along the [001] direction (Figure S18).

(S_{Fc})-**11a** and (S_{Fc})-**12a** are isomers, differing in the position of the phenyl group on the substituted cyclopentadienyl ring. Although these two structures display similar in-plane areas per molecule (Table S11), their molecular planes containing the I···C motif differ in the orientations of the molecules within them (Figures S10 and S13) and in somewhat different plane thicknesses (Table S11), making these two structures less superimposable than are (S_{Fc})-**11a** and (S_{Fc})-**11b** (phenyl/naphthyl substitution).

(S_{Fc})-**9c** and **9c** crystallize in the $P2_12_12_1$ and $Pnma$ space groups, respectively. Their crystal structures only differ in the ordering of the fluorine position in enantiopure (S_{Fc})-**9c** with respect to the F/H site position disorder observed for the racemic **9c**.

(S_{Fc})-**11b** and its racemic counterpart **11b** have also similar crystal packings to some extent. Although the molecular orientations differ, leading to different plane thicknesses (Table S11), the more pronounced interplane penetration found in (S_{Fc})-**11b** leads finally to a similar packing when the barycenter of ferrocenyl groups is considered (Figure S20).

In addition to these eight crystal structures sharing similar molecular plane packings, the methyl-substituted derivative **13** exhibits an interesting further level of sophistication in its structure. Indeed, the halogen I···C interactions form interpenetrated helices of reversed chirality parallel to the [010] direction (Figure 2).

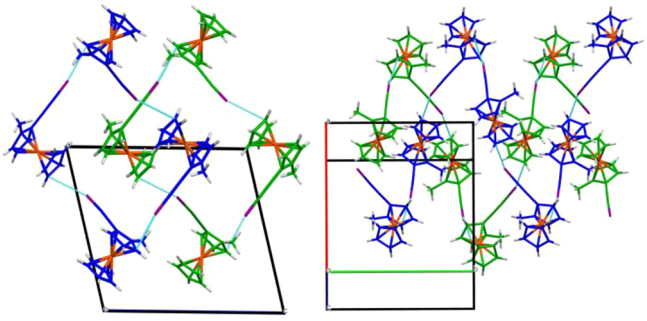

Figure 2. Views along [010] (left) and [001]* (right) of the infinite chains made of I···C halogen bonds (shown in dashed cyan) forming interpenetrating helices (highlighted in blue and green) in **13**.

CONCLUSION

Two series of chiral σ-hole bond donors based on the ferrocenyl ethynyl scaffold were prepared and studied. In these systems, the direct attachment of the donor atoms (I, S, Se) to the alkyne function allows increasing their σ-hole depth. Representative compounds of each series of these new chiral σ-hole bond donors were used in solution for the activation of either a C−Br bond in a Ritter reaction or a thioamide for the synthesis of benzoxazole. Whereas the Se-based compound

https://dx.doi.org/10.1021/acs.organomet.0c00633
Organometallics XXXX, XXX, XXX−XXX

furnished low or no conversion, the ferrocenyl iodoalkyne derivatives generally showed a very good activity in both reactions. Therefore, in view of the develpoment of enantiopure XB-based organocatalysts, the asymmetric synthesis of 1,2- and 1,3-disubstituted ferrocenyl iodoalkynes was performed with functional group introduction in 2- or 3-positions of different natures. The crystal structures of some derivatives in racemic or enantiopure forms were analyzed, confirming their good σ-hole bond donor property also in the solid state. Indeed, several intermolecular contacts between the electropositive σ hole of the iodine atom and electron-rich π clouds were noticed, such as the C−C triple bond and the Cp ring. The search for asymmetric reactions catalyzed by appropriately decorated enantiopure ferrocenyl iodoalkynes is currently underway in our laboratory.

EXPERIMENTAL SECTION

General Information. Proton (^{1}H NMR) and carbon (^{13}C NMR) nuclear magnetic resonance spectra were recorded on a 300, 400, or 500 MHz instrument. The chemical shifts are given in parts per million (ppm) on the δ scale. The solvent peak was used as a reference value: for ^{1}H NMR, $CDCl_3$ at 7.26 ppm; for ^{13}C NMR, $CDCl_3$ at 77.16 ppm. Data are presented as follows: chemical shift, multiplicity (s = singlet, d = doublet, t = triplet, q = quartet, quint = quintet, m = multiplet, b = broad), integration, and coupling constants (J/Hz). High-resolution mass spectra (HRMS) data were recorded on a micrOTOF spectrometer equipped with an orthogonal electrospray interface (ESI). $[\alpha]_D$ values were measured at the sodium D line on a JASCO J-815 CD spectropolarimeter, in $CHCl_3$ in a quartz cuvette (1 cm) at 20 °C. Melting points were obtained in open capillary tubes and are uncorrected. Analytical thin-layer chromatography (TLC) was carried out on silica gel 60 F254 plates with visualization by ultraviolet light. Reagents and solvents were purified using standard means. Tetrahydrofuran (THF) was distilled from sodium metal/benzophenone and used fresh. Anhydrous toluene, acetonitrile, and MeOH were obtained by passing through activated alumina under a positive pressure of argon using GlassTechnology GTS100 devices. Diisopropylamine was distilled over CaH_2 and stored over KOH, under an argon atmosphere. Anhydrous reactions were carried out in flame-dried glassware and under an argon atmosphere. All other chemicals were used as received.

Computational Details. The 3D structures of selected compounds (see Table 1) were optimized at the DFT level of theory using the B3LYP functional (completed with D3 dispersion corrections) and the Def2TZVPP basis set. Conformations were searched by scanning the corresponding degrees of freedom, and frequency calculations were performed in order to check that true energy minima were obtained. The computations of the electrostatic potential mapped on 0.002 au electron density isosurfaces and searches for extrema $V_{S,max}$ were performed with the AIMAll[77] and MultiWfn programs.[78,79]

HPLC on Chiral Stationary Phase. An Agilent Technologies (Waldbronn, Germany) 1100 Series HPLC system (high-pressure binary gradient system equipped with a diode-array detector operating at multiple wavelengths (220, 254, 280 nm), a programmable autosampler with a 20 μL loop, and a thermostated column compartment) was employed for analytical enantioseparations. Data acquisition and analyses were carried out with Agilent Technologies ChemStation Version B.04.03 chromatographic data software. The UV absorbance is reported as milliabsorbance units (mAU). Lux Cellulose-1 (coated cellulose tris(3,5-dimethylphenylcarbamate)), i-Cellulose-5 (immobilized tris(3,5-dichlorophenylcarbamate)), and i-Amylose-3 (immobilized amylose tris(3-chloro-5-methylphenylcarbamate)) (Phenomenex Inc., Torrance, CA, USA) were used as chiral columns (250 × 4.6 mm; 5 μm). i-Cellulose-5 and i-Amylose-3 were kindly provided by Prof. Bezhan Chankvetdze, University of Tbilisi (Tbilisi, Georgia). HPLC-grade n-heptane, n-hexane, methanol, and 2-propanol were purchased and used as received. Analyses were performed at a flow rate of 0.8 mL/min and 22 °C.

General Procedures for the Sonogashira Reaction. *Conditions A.* To the substituted iodoferrocene **1** or **2** (1 equiv) under argon were successively added degassed diisopropylamine (5 mL/mmol), $Pd(PPh_3)_4$ (5 mol %), and CuI (10 mol %). After the mixture was stirred at room temperature for 5 min, trimethylsilylacetylene (3 equiv) was added and the mixture was heated at 60 °C and stirred for 15 h. After the mixture was cooled to room temperature, it was filtered over Celite and washed with dichloromethane. The filtrate was washed with water, and the organic phase was collected and dried over Na_2SO_4. After filtration and concentration, the crude product was purified by chromatography on silica gel (pentane or pentane/Et_2O 98/2) to give the expected product.

Conditions B. In a flask containing iodoferrocene **1** or **2** (1 equiv), $Pd(\text{-}Pt\text{-}Bu_3)_2$ (3 mol %), and CuI (3 mol %) were placed a degassed THF/iPr$_2$NH 3/1 mixture (1.5 mL/mmol) and finally trimethylsilylacetylene (2 equiv). After it was stirred at room temperature for 20 h, the mixture was filtered over Celite and washed with dichloromethane. After concentration, the crude product was purified by chromatography on silica gel (pentane or pentane/Et_2O 98/2) to give the expected product.

*((2-Bromoferrocenyl)ethynyl)trimethylsilane (**4a**).* Conditions A: **4a** (3.04 g, 98%) obtained from **1a** (8.57 mmol, 3.35 g). Conditions B: **4a** (115 mg, 89%) obtained from **1a** (0.358 mmol, 140 mg). Red solid. Mp: 38−40 °C. ^{1}H NMR (500 MHz, $CDCl_3$): δ 4.47 (s, 1H), 4.41 (s, 1H), 4.23 (s, 5H), 4.14 (s, 1H), 0.26 (s, 9H). ^{13}C NMR (126 MHz, $CDCl_3$): δ 101.7, 94.5, 81.0, 72.9, 70.8, 70.2, 67.3, 67.0, 0.3. HRMS (ESI-TOF): m/z $[M]^+$ calcd for $C_{15}H_{17}BrFeSi$ 359.9627; found 359.9613.

*((2-Chloroferrocenyl)ethynyl)trimethylsilane (**4b**).* Conditions A: **4b** (540 mg, 62%) obtained from **1b** (2.77 mmol, 960 mg). Conditions B: **4b** (82 mg, 94%) obtained from **1b** (0.277 mmol, 96 mg). Red solid. Mp: 45−47 °C. ^{1}H NMR (500 MHz, $CDCl_3$): δ 4.45 (m, 1H), 4.37 (m, 1H), 4.24 (s, 5H), 4.08 (m, 1H), 0.27 (s, 9H). ^{13}C NMR (126 MHz, $CDCl_3$): δ 100.9, 94.7, 94.5, 72.5, 69.5, 68.4, 66.0, 65.1, 0.3. HRMS (ESI-TOF): m/z $[M]^+$ calcd for $C_{15}H_{17}ClFeSi$ 316.0132; found 316.0143.

*((2-Fluoroferrocenyl)ethynyl)trimethylsilane (**4c**).* Conditions A: **4c** (127 mg, 42%) obtained from **1c** (1 mmol, 330 mg). Conditions B: **4c** (49 mg, 46%) obtained from **1c** (0.352 mmol, 116 mg) (50 mg of starting material was recovered). Red oil. ^{1}H NMR (500 MHz, $CDCl_3$): δ 4.35 (s, 1H), 4.28 (s, 5H), 4.11 (s, 1H), 3.82 (s, 1H), 0.25 (s, 9H). ^{13}C NMR (126 MHz, $CDCl_3$): δ 135.4 (d, J = 274.9 Hz), 99.5 (d, J = 3.8 Hz), 94.4, 71.6, 65.3 (d, J = 2.5 Hz), 60.9 (d, J = 3.8 Hz), 56.5 (d, J = 13.9 Hz), 54.6 (d, J = 12.6 Hz), 0.3. ^{19}F NMR (75 MHz, $CDCl_3$): δ −186.7. HRMS (ESI-TOF): m/z $[M]^+$ calcd for $C_{15}H_{17}FFeSi$ 300.0427; found 300.0424.

*2-((Trimethylsilyl)ethynyl)cyanoferrocene (**4d**).* Conditions A: **4d** obtained from **1d** (0.816 mmol, 275 mg) as a 3:2 mixture with cyanoferrocene (180 mg). Conditions B: **4d** (20 mg, 55%) obtained from **1d** (0.118 mmol, 39.6 mg). Red oil. ^{1}H NMR (500 MHz, $CDCl_3$): δ 4.66 (bs, 1H), 4.63 (bs, 1H), 4.39 (t, J = 2.5 Hz, 1H), 4.36 (s, 5H), 0.25 (s, 9H). ^{13}C NMR (126 MHz, $CDCl_3$): δ 118.8, 99.3, 96.2, 73.8, 72.9, 72.1, 70.8, 69.4, 55.8, 0.2. HRMS (ESI-TOF): m/z $[M]^+$ calcd for $C_{16}H_{17}FeNSi$ 307.0474; found 307.0455.

*((3-Bromoferrocenyl)ethynyl)trimethylsilane (**5a**).* Conditions A: **5a** (176 mg, 48%) obtained from **2a** (1.023 mmol, 400 mg). Conditions B: **5a** (118 mg, 91%) obtained from **2a** (0.358 mmol, 140 mg). Red solid. Mp: 58−60 °C. ^{1}H NMR (500 MHz, $CDCl_3$): δ 4.69 (m, 1H), 4.43 (m, 1H), 4.37 (m, 1H), 4.26 (s, 5H), 0.21 (s, 9H). ^{13}C NMR (126 MHz, $CDCl_3$): δ 102.5, 92.1, 77.2, 73.5, 72.8, 71.0, 70.8, 64.6, 0.3. HRMS (ESI-TOF): m/z $[M]^+$ calcd for $C_{15}H_{17}BrFeSi$ 359.9627; found 359.9619.

*((3-Chloroferrocenyl)ethynyl)trimethylsilane (**5b**).* Conditions A: **5b** (55 mg, 38%) obtained from **2b** (0.462 mmol, 160 mg). Conditions B: **5b** (134 mg, 92%) obtained from **2b** (0.462 mmol, 160 mg). Red oil. ^{1}H NMR (500 MHz, $CDCl_3$): δ 4.67 (s, 1H), 4.40 (m, 1H), 4.33 (s, 1H), 4.27 (s, 5H), 0.21 (s, 9H). ^{13}C NMR (126 MHz, $CDCl_3$): δ 102.6, 92.2, 91.8, 72.5, 71.3, 69.8, 68.7, 63.5, 0.3. HRMS

https://dx.doi.org/10.1021/acs.organomet.0c00633
Organometallics XXXX, XXX, XXX−XXX

(ESI-TOF): m/z $[M]^+$ calcd for $C_{15}H_{17}ClFeSi$ 316.0132; found 316.0140.

*((3-Fluoroferrocenyl)ethynyl)trimethylsilane (**5c**).* Conditions A: **5c** (46 mg, 31%) obtained from **2c** (0.5 mmol, 165 mg). Conditions B: **5c** (111 mg, 74%) obtained from **2c** (0.5 mmol, 165 mg). Red oil. ^{1}H NMR (500 MHz, $CDCl_3$): δ 4.60 (s, 1H), 4.34 (s, 1H), 4.30 (s, 5H), 4.11 (s, 1H), 0.21 (s, 9H). ^{13}C NMR (126 MHz, $CDCl_3$): δ 134.6 (d, J = 270.9 Hz), 103.2, 91.1, 71.7, 65.0, 59.6 (d, J = 15.1 Hz), 58.5 (d, J = 5.0 Hz), 57.0 (d, J = 15.1 Hz), 0.3. ^{19}F NMR (75 MHz, $CDCl_3$): δ −186.1. HRMS (ESI-TOF): m/z $[M]^+$ calcd for $C_{15}H_{17}FFeSi$ 300.0427; found 300.0435.

General Procedure for Aldehyde Homologation. Ferrocenecarboxaldehyde (S_{Fc})-**36** or (S_{Fc})-**39** (1 equiv) was dissolved in THF (3 mL/mmol), and the temperature was lowered to 0 °C. A solution of diazophosphonate **38** (1.2 equiv) in MeOH (2.5 mL/mmol) was added, followed by K_2CO_3 (2.2 equiv). The temperature was raised to room temperature, and the mixture was stirred for 15 h. After concentration, the crude product was extracted with Et_2O and the extract washed with water and brine. The organic phases were collected, dried over Na_2SO_4, and concentrated. The crude product was purified by chromatography on silica gel (pentane/Et_2O 4/1) to give the expected product.

*(S_{Fc})-1-Bromo-2-ethynylferrocene ((S_{Fc})-**37**).* Red oil (1.59 g, 89%) obtained from (S_{Fc})-**36** (6.14 mmol, 1.8 g). ^{1}H NMR (500 MHz, $CDCl_3$): δ 4.50 (bs, 1H), 4.45 (bs, 1H), 4.26 (s, 5H), 4.17 (t, J = 2.5 Hz, 1H), 2.94 (s, 1H). ^{13}C NMR (126 MHz, $CDCl_3$): δ 80.8, 80.5, 76.8, 72.8, 70.9, 70.5, 67.4, 66.0. $[\alpha]_D^{20}$ = +21 (c = 0.7, $CHCl_3$). HRMS (ESI-TOF): m/z $[M]^+$ calcd for $C_{12}H_9BrFe$ 287.9232; found 287.9228.

*(S_{Fc})-1-Ethynyl-3-iodoferrocene ((S_{Fc})-**40**).* Red oil (460 mg, 86%) obtained from (S_{Fc})-**39** (1.59 mmol, 540 mg). ^{1}H NMR (500 MHz, $CDCl_3$): δ 4.72 (bs, 1H), 4.453 (s, 1H), 4.451 (s, 1H), 4.25 (s, 5H), 2.77 (s, 1H); ^{13}C NMR (126 MHz, $CDCl_3$): δ 81.0, 77.8, 75.4, 75.1, 73.1, 72.6, 65.3, 38.9. $[\alpha]_D^{20}$ = +125 (c = 0.5, $CHCl_3$). HRMS (ESI-TOF): m/z $[M]^+$ calcd for $C_{12}H_9FeI$ 335.9093; found 335.9083.

General Procedure for TMS Protection. To a solution of ethynylferrocene (S_{Fc})-**37** or (S_{Fc})-**40** (1 equiv) at −78 °C was added a freshly prepared solution of LiHMDS (1 M in THF, 1.5 equiv), and the mixture was stirred for 30 min at −78 °C. TMSCl (1.5 equiv) was added, and stirring was continued for 30 min at −78 °C before the temperature was raised to ambient. A saturated solution of NH_4Cl was added, and the mixture was extracted with Et_2O and the extract washed with water. After drying the organic phase over Na_2SO_4, it was filtered and concentrated. The crude was purified by chromatography on silica gel (pentane/Et_2O 8/1) to give the expected product.

*(S_{Fc})-((2-Bromoferrocenyl)ethynyl)trimethylsilane ((S_{Fc})-**4a**).* Red oil (1.75 g, 99%) obtained from (S_{Fc})-**37** (4.84 mmol, 1.4 g). $[\alpha]_D^{20}$ = −16 (c = 0.7, $CHCl_3$). HRMS (ESI-TOF): m/z $[M]^+$ calcd for $C_{15}H_{17}BrFeSi$ 359.9627; found 359.9637.

*(S_{Fc})-((3-Iodoferrocenyl)ethynyl)trimethylsilane ((S_{Fc})-**41**).* Red solid (540 mg, 99%) obtained from (S_{Fc})-**40** (1.335 mmol, 450 mg). Mp: 50−52 °C. ^{1}H NMR (500 MHz, $CDCl_3$): δ 4.69 (s, 1H), 4.43 (s, 1H), 4.41 (s, 1H), 4.22 (s, 5H), 0.22 (s, 9H). ^{13}C NMR (126 MHz, $CDCl_3$): δ 102.4, 92.3, 77.8, 75.3, 73.2, 72.5, 66.3, 39.1, 0.3. $[\alpha]_D^{20}$ = +126 (c = 0.6, $CHCl_3$). HRMS (ESI-TOF): m/z $[M]^+$ calcd for $C_{15}H_{17}FeISi$ 407.9488; found 407.9486.

General Procedure for the Suzuki Reaction. Haloferrocene **4a**, **5a**, or (S_{Fc})-**41** (1 equiv), Pd_2dba_3 (2 mol %), SPhos (4 mol %), boronic acid (1.5 equiv), and crushed K_3PO_4 (3 equiv) were placed in a Schlenk tube under argon. Degassed toluene (3 mL/mmol) was added, and the mixture was heated at 100 °C and stirred for 15 h. After it was cooled to room temperature, the mixture was filtered over Celite and washed with ethyl acetate. The filtrate was concentrated and purified by chromatography on silica gel (pentane or pentane/Et_2O 98/2) to give the expected product.

*Trimethyl((2-phenylferrocenyl)ethynyl)silane (**6a**).* Red solid (1.05 g, 98%) obtained from **4a** (3 mmol, 1.08 g). Mp: 46−48 °C. ^{1}H NMR (500 MHz, $CDCl_3$): δ 7.87 (d, J = 7.0 Hz, 2H), 7.35 (t, J = 7.0 Hz, 2H), 7.27 (t, J = 7.0 Hz, 1H), 4.63 (m, 1H), 4.61 (m, 1H), 4.33 (t, J = 3.0 Hz, 1H), 4.13 (s, 5H), 0.27 (s, 9H). ^{13}C NMR (126 MHz, $CDCl_3$): δ 138.0, 128.0, 127.9, 126.6, 104.7, 93.8, 87.9, 73.0, 71.9, 68.6, 68.5, 63.9, 0.2. HRMS (ESI-TOF): m/z $[M]^+$ calcd for $C_{21}H_{22}FeSi$ 358.0835; found 358.0823.

*(S_{Fc})-Trimethyl((2-phenylferrocenyl)ethynyl)silane ((S_{Fc})-**6a**).* Red oil (160 mg, 89%) obtained from (S_{Fc})-**4a** (0.5 mmol, 180 mg). $[\alpha]_D^{20}$ = −16 (c = 0.5, $CHCl_3$). HRMS (ESI-TOF): m/z $[M]^+$ calcd for $C_{21}H_{22}FeSi$ 358.0835; found 358.0829.

*Trimethyl((2-(naphthalen-2-yl)ferrocenyl)ethynyl)silane (**6b**).* Red oil (572 mg, 93%) obtained from **4a** (1.5 mmol, 542 mg). ^{1}H NMR (500 MHz, $CDCl_3$): δ 8.33 (s, 1H), 8.00 (dd, J = 8.5, 1.5 Hz, 1H), 7.83 (m, 3H), 7.47 (m, 2H), 4.74 (m, 1H), 4.65 (m, 1H), 4.38 (t, J = 3.0 Hz, 1H), 4.13 (s, 5H), 0.29 (s, 9H). ^{13}C NMR (126 MHz, $CDCl_3$): δ 135.6, 133.5, 132.4, 127.85, 127.8, 127.4, 126.7, 126.3, 125.8, 125.6, 104.7, 93.9, 87.5, 73.4, 71.9, 68.85, 68.8, 63.9, 0.3. HRMS (ESI-TOF): m/z $[M]^+$ calcd for $C_{25}H_{24}FeSi$ 408.0991; found 408.0997.

*(S_{Fc})-Trimethyl((2-(naphthalen-2-yl)ferrocenyl)ethynyl)silane ((S_{Fc})-**6b**).* Red oil (200 mg, 98%) obtained from (S_{Fc})-**4a** (0.5 mmol, 180 mg). $[\alpha]_D^{20}$ = +107 (c = 0.5, $CHCl_3$). HRMS (ESI-TOF): m/z $[M]^+$ calcd for $C_{25}H_{24}FeSi$ 408.0991; found 408.0971.

*Trimethyl((3-phenylferrocenyl)ethynyl)silane (**7a**).* Red solid (60 mg, 82%) obtained from **5a** (0.208 mmol, 75 mg). Mp: 120−122 °C. ^{1}H NMR (500 MHz, $CDCl_3$): δ 7.45 (d, J = 7.0 Hz, 2H), 7.30 (t, J = 7.0 Hz, 2H), 7.21 (t, J = 7.0 Hz, 1H), 4.93 (m, 1H), 4.66 (m, 1H), 4.58 (m, 1H), 4.09 (s, 5H), 0.25 (s, 9H). ^{13}C NMR (126 MHz, $CDCl_3$): δ 138.3, 128.6, 126.5, 126.3, 104.0, 91.2, 86.3, 72.6, 71.8, 70.1, 67.3, 65.8, 0.4. HRMS (ESI-TOF): m/z $[M]^+$ calcd for calcd for $C_{21}H_{22}FeSi$ 358.0835; found 358.0843.

*(S_{Fc})-Trimethyl((3-phenylferrocenyl)ethynyl)silane ((S_{Fc})-**7a**).* Red solid (130 mg, 84%) obtained from (S_{Fc})-**41** (0.43 mmol, 175 mg). Mp: 142−144 °C. $[\alpha]_D^{20}$ = +65 (c = 0.5, $CHCl_3$). HRMS (ESI-TOF): m/z $[M]^+$ calcd for $C_{21}H_{22}FeSi$ 358.0835; found 358.0837.

*Trimethyl((3-(naphthalen-2-yl)ferrocenyl)ethynyl)silane (**7b**).* Red solid (46 mg, 80%) obtained from **5a** (0.141 mmol, 51 mg). Mp: 85−87 °C. ^{1}H NMR (500 MHz, $CDCl_3$): δ 7.86 (s, 1H), 7.79 (m, 3H), 7.61 (dd, J = 8.5, 1.5 Hz, 1H), 7.46 (m, 2H), 5.07 (m, 1H), 4.79 (m, 1H), 4.65 (t, J = 3.0 Hz, 1H), 4.10 (s, 5H), 0.26 (s, 9H). ^{13}C NMR (126 MHz, $CDCl_3$): δ 135.8, 133.7, 132.4, 128.1, 127.9, 127.7, 126.5, 125.6, 125.2, 124.0, 103.9, 91.3, 86.1, 72.8, 71.9, 70.3, 67.4, 66.1, 0.4. HRMS (ESI-TOF): m/z $[M]^+$ calcd for $C_{25}H_{24}FeSi$ 408.0991; found 408.0994.

*(S_{Fc})-Trimethyl((3-(naphthalen-2-yl)ferrocenyl)ethynyl)silane ((S_{Fc})-**7b**).* Red solid (150 mg, 85%) obtained from (S_{Fc})-**41** (0.43 mmol, 175 mg). Mp: 95−97 °C. $[\alpha]_D^{20}$ = +131 (c = 0.7, $CHCl_3$). HRMS (ESI-TOF): m/z $[M]^+$ calcd for $C_{25}H_{24}FeSi$ 408.0991; found 408.0991.

General Procedure for the Lithiation/Electrophilic Trapping. To a solution of **4a** or (S_{Fc})-**4a** (1 equiv) in THF (5 mL/mmol) at −78 °C was slowly added *n*-BuLi (1.4 M in hexanes, 1.2 equiv), and the mixture was stirred at −78 °C for 1 h. An electrophile (1.2 equiv) was added, and stirring was continued at −78 °C for 1 h. The temperature was raised to 0 °C before the mixture was quenched with a saturated solution of NH_4Cl. The mixture was extracted with ethyl acetate and the extract washed with water and brine. After drying over Na_2SO_4, filtration, and concentration, the crude product was purified by chromatography on silica gel (pentane/Et_2O 98/2) to give the expected product.

*Trimethyl((2-methylferrocenyl)ethynyl)silane (**8**).* Red oil (208 mg, 70%) obtained by using 1 mmol of **4a** and 1.2 mmol of MeI (neat) as the electrophile. ^{1}H NMR (500 MHz, $CDCl_3$): δ 4.34 (m, 1H), 4.14 (m, 1H), 4.09 (s, 5H), 4.04 (t, J = 2.5 Hz, 1H), 2.08 (s, 3H), 0.24 (s, 9H). ^{13}C NMR (126 MHz, $CDCl_3$): δ 104.0, 92.5, 87.0, 70.9, 70.6, 69.7, 67.1, 65.8, 13.7, 0.5. HRMS (ESI-TOF): m/z $[M]^+$ calcd for $C_{16}H_{20}FeSi$ 296.0678; found 296.0671.

*(R_{Fc})-Trimethyl((2-methylferrocenyl)ethynyl)silane ((R_{Fc})-**8**).* Red solid (120 mg, 73%) obtained by using by using 0.55 mmol of **4a** and 0.66 mmol of MeI (neat) as the electrophile. Mp: 33−35 °C. $[\alpha]_D^{20}$ = −49 (c = 0.3, $CHCl_3$). HRMS (ESI-TOF): m/z $[M]^+$ calcd for $C_{16}H_{20}FeSi$ 296.0678; found 296.0662.

https://dx.doi.org/10.1021/acs.organomet.0c00633
Organometallics XXXX, XXX, XXX−XXX

*(S_{Fc})-((2-Fluoroferrocenyl)ethynyl)trimethylsilane ((S_{Fc})-**4c**).* Red oil (118 mg, 71%) obtained by using 0.55 mmol of **4a** and 0.66 mmol of NFSI (solid) as the electrophile. $[\alpha]_D^{20} = -4$ (c = 1.4, $CHCl_3$). HRMS (ESI-TOF): m/z $[M]^+$ calcd for $C_{15}H_{17}FFeSi$ 300.0427; found 300.0431.

*(S_{Fc})-2-((Trimethylsilyl)ethynyl)cyanoferrocene ((S_{Fc})-**4d**).* Red oil (70 mg, 41%) obtained by using 0.55 mmol of **4a** and 0.66 mmol of TsCN (in THF) as the electrophile. $[\alpha]_D^{20} = -37$ (c = 0.2, $CHCl_3$). HRMS (ESI-TOF): m/z $[M]^+$ calcd for $C_{16}H_{17}FeNSi$ 307.0474; found 307.0465.

*(S_{Fc})-((3-Bromoferrocenyl)ethynyl)trimethylsilane ((S_{Fc})-**5a**).* (S_{Fc})-**41** (0.452 mmol, 185 mg) was dissolved in THF (3 mL), and the solution was cooled to −78 °C. *t*-BuLi (1.7 M in pentane, 0.95 mmol, 0.56 mL) was slowly added, and the mixture was stirred at −78 °C for 30 min. A solution of α,α'-dibromoxylene (0.54 mmol, 140 mg) in THF (2 mL) was added, and stirring was continued for 30 min. The temperature was raised to ambient temperature, and water (0.5 mL) was slowly added. After filtration on Celite (Et_2O), the organic phase was separated and dried over Na_2SO_4. After filtration and concentration, the crude product was purified by chromatography on silica gel (pentane) to give a red solid (150 mg) with a ^1H NMR spectrum similar to that of racemic **5a**. However, it contained some inseparable impurities and was used without further purification in the next step.

General Procedures for the Deprotection−Iodination. *Conditions a.* The ferrocenyl ethynyltrimethylsilane (1 equiv) was dissolved in acetonitrile (10 mL/mmol) and placed in the dark at room temperature. AgF (1.1 equiv) and NIS (1.1 equiv) were successively added, and the mixture was stirred for 15 h. After filtration over Celite (Et_2O) and concentration, the crude product was purified by chromatography on silica gel (pentane or pentane/Et_2O 98/2) to give the expected product.

Conditions b. The ferrocenyl ethynyltrimethylsilane (1 equiv) was dissolved in methanol (15 mL/mmol) and the solution was cooled to 0 °C. Crushed KOH (2.5 equiv) was added, and the mixture was stirred at 0 °C for 5 min and at room temperature for 2 h. Diethyl ether was added, and the mixture was washed with water and then with brine. The organic phase was extracted, dried over Na_2SO_4, filtered, and concentrated. The crude product was purified by chromatography on silica gel (pentane/Et_2O 99/1) to give the free alkynes.

*1-Chloro-2-ethynylferrocene (**14**).* Compound **14** (red oil, 25 mg, 79%) obtained from **4b** (0.13 mmol, 41 mg) and KOH (0.325 mmol, 18.2 mg) in MeOH (2 mL). ^1H NMR (500 MHz, $CDCl_3$): δ 4.47 (br s, 1H), 4.40 (br s, 1H), 4.27 (s, 5H), 4.11 (t, J = 2.5 Hz, 1H), 2.95 (s, 1H). ^{13}C NMR (126 MHz, $CDCl_3$): δ 94.5, 79.7, 72.5, 69.7, 68.5, 66.1, 64.1. HRMS (ESI-TOF): m/z $[M]^+$ calcd for $C_{12}H_9ClFe$ 243.9737; found 243.9750.

*1-Chloro-3-ethynylferrocene (**15**).* Compound **15** (red oil, 46 mg, 87%) obtained from compound **5b** (0.212 mmol, 67 mg) and KOH (0.529 mmol, 29.6 mg) in MeOH (3.2 mL). ^1H NMR (500 MHz, $CDCl_3$): δ 4.69 (br s, 1H), 4.43 (br s, 1H), 4.36 (br s, 1H), 4.29 (s, 5H), 2.71 (s, 1H). ^{13}C NMR (126 MHz, $CDCl_3$): δ 92.2, 81.3, 74.6, 72.4, 71.3, 69.8, 68.7. HRMS (ESI-TOF): m/z $[M]^+$ calcd for $C_{12}H_9ClFe$ 243.9737; found 243.9756.

Conditions c. The free alkynylferrocene (1 equiv) was dissolved in methanol (15 mL/mmol), and the solution was cooled to 0 °C. Crushed KOH (2.5 equiv) was added, and the mixture was stirred at 0 °C for 15 min. NIS (1.5 equiv) was added, and the mixture was stirred for 5 min at 0 °C and then for 2 h at room temperature. Diethyl ether was added, and the mixture was washed with water and then with brine. The organic phase was extracted, dried over Na_2SO_4, filtered, and concentrated. The crude product was purified by chromatography on silica gel (pentane/Et_2O 99/1) to give the iodoalkynes.

Conditions d (One Pot). The ferrocenyl ethynyltrimethylsilane (1 equiv) was dissolved in methanol (15 mL/mmol), and the solution was cooled to 0 °C. Crushed KOH (5 equiv) was added, and the mixture was stirred at 0 °C for 5 min and at room temperature for 2 h. After the mixture was cooled to 0 °C, NIS (1.5 equiv) was added and the mixture was stirred for 5 min at 0 °C and then for 2 h at room temperature. Diethyl ether was added, and the mixture was washed with water and then with brine. The organic phase was extracted, dried over Na_2SO_4, filtered, and concentrated. The crude product was purified by chromatography on silica gel (pentane/Et_2O 99/1) to give the iodoalkynes.

*1-Bromo-2-(iodoethynyl)ferrocene (**9a**).* Conditions a: **9a** (82 mg, 56%) obtained from **4a** (0.354 mmol, 128 mg). Conditions d: **9a** (49 mg, 71%) obtained from **4a** (0.166 mmol, 60 mg). Red solid. Mp: 70−72 °C. ^1H NMR (500 MHz, $CDCl_3$): δ 4.48 (m, 1H), 4.43 (m, 1H), 4.27 (s, 5H), 4.15 (t, J = 2.5 Hz, 1H). ^{13}C NMR (126 MHz, $CDCl_3$): δ 89.9, 80.9, 72.7, 70.7, 70.5, 67.7, 67.3, 3.5. HRMS (ESI-TOF): m/z $[M]^+$ calcd for $C_{12}H_8BrFeI$ 413.8198; found 413.8202.

*(S_{Fc})-1-Bromo-2-(iodoethynyl)ferrocene ((S_{Fc})-**9a**).* Conditions a: (61 mg, 53%) obtained from (S_{Fc})-**4a** (0.277 mmol, 100 mg). Conditions d: **9a** (36 mg, 87%) obtained from (S_{Fc})-**4a** (0.1 mmol, 36 mg). Red solid. Mp: 99−101 °C. $[\alpha]_D^{20} = +12$ (c = 0.6, $CHCl_3$). HRMS (ESI-TOF): m/z $[M]^+$ calcd for $C_{12}H_8BrFeIi$ 413.8198; found 413.8102.

*1-Chloro-2-(iodoethynyl)ferrocene (**9b**).* Conditions a: **9b** (124 mg, 48%) obtained from **4b** (0.695 mmol, 220 mg). Conditions c: **9b** (25 mg, 72%) obtained from **14** (0.094 mmol, 23 mg); Conditions d: **9b** (37 mg, 77%) obtained from **4b** (0.13 mmol, 41 mg). Red solid. Mp: 80−82 °C. ^1H NMR (500 MHz, $CDCl_3$): δ 4.45 (m, 1H), 4.38 (m, 1H), 4.28 (s, 5H), 4.09 (t, J = 2.5 Hz, 1H). ^{13}C NMR (126 MHz, $CDCl_3$): δ 94.7, 89.2, 72.4, 69.7, 68.4, 66.0, 65.8, 3.7. HRMS (ESI-TOF): m/z $[M]^+$ calcd for $C_{12}H_8ClFeI$ 369.8703; found 369.8705.

*1-Fluoro-2-(iodoethynyl)ferrocene (**9c**).* Conditions a: **9c** (25 mg, 42%) obtained from **4c** (0.167 mmol, 50 mg), Conditions d: **9c** (54 mg, 93%) obtained from **4c** (0.163 mmol, 49 mg). Red solid. Mp: 63−65 °C. ^1H NMR (500 MHz, $CDCl_3$): δ 4.36 (m, 1H), 4.31 (s, 5H), 4.12 (m, 1H), 3.84 (m, 1H). ^{13}C NMR (126 MHz, $CDCl_3$): δ 135.8 (d, J = 275.9 Hz), 87.8 (d, J = 3.8 Hz), 71.4, 65.2 (d, J = 1.3 Hz), 60.9 (d, J = 4.0 Hz), 56.4 (d, J = 13.9 Hz), 55.3 (d, J = 12.6 Hz), 3.5. ^{19}F NMR (75 MHz, $CDCl_3$): δ −186.7. HRMS (ESI-TOF): m/z $[M]^+$ calcd for $C_{12}H_8FFeI$ 353.8999; found 353.9000.

*(S_{Fc})-1-Fluoro-2-(iodoethynyl)ferrocene ((S_{Fc})-**9c**).* Conditions a: (S_{Fc})-**9c** (59 mg, 51%) obtained from (S_{Fc})-**4c** (0.327 mmol, 98 mg). Red solid. Mp: 107−109 °C. $[\alpha]_D^{20} = -10$ (c = 0.44, $CHCl_3$). HRMS (ESI-TOF): m/z $[M]^+$ calcd for $C_{12}H_8FFeI$ 353.8999; found 353.8983.

*2-(Iodoethynyl)cyanoferrocene (**9d**).* Conditions d: **9d** (20 mg, 85%) obtained from **4d** (20 mg, 0.065 mmol). Light-sensitive red solid. Mp: 119−121 °C. ^1H NMR (500 MHz, $CDCl_3$): δ 4.67 (m, 1H), 4.65 (m, 1H), 4.41 (m, 1H), 4.40 (s, 5H). ^{13}C NMR (126 MHz, $CDCl_3$): δ 118.8, 87.8, 74.1, 72.1, 70.8, 70.0, 55.8, 6.6. HRMS (ESI-TOF): m/z $[M]^+$ calcd for $C_{13}H_8FeIN$ 360.9045; found 360.9037.

*(S_{Fc})-2-(Iodoethynyl)cyanoferrocene ((S_{Fc})-**9d**).* Conditions a: (S_{Fc})-**9d** (60 mg, 77%) obtained from (S_{Fc})-**4d** (0.217 mmol, 67 mg). Light-sensitive red solid. Mp: 150−152 °C. $[\alpha]_D^{20} = +65$ (c = 0.5, $CHCl_3$). HRMS (ESI-TOF): m/z $[M]^+$ calcd for $C_{13}H_8FeIN$ 360.9045; found 360.9042.

*1-Bromo-3-(iodoethynyl)ferrocene (**10a**).* Conditions a: **10a** (24 mg, 84%) obtained from **5a** (0.069 mmol, 25 mg). Red oil. ^1H NMR (500 MHz, $CDCl_3$): δ 4.69 (br s, 1H), 4.44 (br s, 1H), 4.38 (br s, 1H), 4.29 (s, 5H). ^{13}C NMR (126 MHz, $CDCl_3$): δ 90.5, 77.0, 73.5, 72.7, 70.9, 65.3, 1.4. HRMS (ESI-TOF): m/z $[M]^+$ calcd for $C_{12}H_8BrFeI$ 413.8200; found 413.8190.

*(S_{Fc})-1-Bromo-3-(iodoethynyl)ferrocene ((S_{Fc})-**10a**).* Conditions a: (S_{Fc})-**10a** (72 mg, 38% for 2 steps) obtained from (S_{Fc})-**41**. Red oil. HRMS (ESI-TOF): m/z $[M]^+$ calcd for $C_{12}H_8BrFeI$ 413.8200; found 413.8188.

*1-Chloro-3-(iodoethynyl)ferrocene (**10b**).* Conditions a: **10b** (29 mg, 50%) obtained from **5b** (0.158 mmol, 50 mg); . Conditions c: **10b** (54 mg, 78%) obtained from **15** (0.188 mmol, 46 mg). Conditions b: **9b** (63 mg, 80%) obtained from **5b** (0.212 mmol, 67 mg). Red oil. ^1H NMR (500 MHz, $CDCl_3$): δ 4.67 (m, 1H), 4.41 (m, 1H), 4.34 (m, 1H), 4.30 (s, 5H); ^{13}C NMR (126 MHz, $CDCl_3$): δ 92.0, 90.7, 72.4, 71.2, 69.9, 68.6, 64.1, 1.1; HRMS (ESI-TOF): m/z $[M]^+$ calcd for $C_{12}H_8ClFe$ 369.8703; found 369.8689.

https://dx.doi.org/10.1021/acs.organomet.0c00633
Organometallics XXXX, XXX, XXX−XXX

*1-Fluoro-3-(iodoethynyl)ferrocene (**10c**).* Conditions a: **10c** (17 mg, 36%) obtained from **4c** (0.133 mmol, 40 mg). Conditions d: **10c** (105 mg, 80%) obtained from **4c** (0.37 mmol, 111 mg). Red oil. ^{1}H NMR (500 MHz, $CDCl_3$): δ 4.60 (m, 1H), 4.34 (m, 1H), 4.32 (s, 5H), 4.12 (m, 1H). ^{13}C NMR (126 MHz, $CDCl_3$): δ 134.2 (d, J = 270.9 Hz), 91.1, 94.4, 71.5, 65.1 (d, J = 2.4 Hz), 59.6 (d, J = 15.0 Hz), 59.2 (d, J = 5.2 Hz), 57.0 (d, J = 14.7 Hz), 0.2. ^{19}F NMR (75 MHz, $CDCl_3$): δ −185.8. HRMS (ESI-TOF): m/z $[M]^+$ calcd for $C_{12}H_8FFe$ 353.8999; found 353.8986.

*1-(Iodoethynyl)-2-phenylferrocene (**11a**).* Conditions a: **11a** (74 mg, 72%) obtained from **6a** (0.25 mmol, 90 mg). Red oil. ^{1}H NMR (500 MHz, $CDCl_3$): δ 7.78 (dd, J = 8.0, 1.5 Hz, 2H), 7.36 (t, J = 8.0 Hz, 2H), 7.28 (dt, J = 7.5, 1.5 Hz, 1H), 4.61 (m, 2H), 4.32 (t, J = 3.0 Hz, 1H), 4.15 (s, 5H). ^{13}C NMR (126 MHz, $CDCl_3$): δ 137.7, 128.2, 127.9, 126.7, 92.1, 88.3, 73.3, 71.7, 68.6, 68.5, 64.7, 2.1. HRMS (ESI-TOF): m/z $[M]^+$ calcd for $C_{18}H_{13}FeI$ 411.9406; found 411.9404.

*(S_{Fc})-1-(Iodoethynyl)-2-phenylferrocene ((S_{Fc})-**11a**).* Conditions a: (S_{Fc})-**11a** (81 mg, 59%) obtained from (S_{Fc})-**6a** (0.335 mmol, 120 mg). Red solid. Mp: 92−94 °C. $[\alpha]_D^{20}$ = +42 (c = 0.4, $CHCl_3$). HRMS (ESI-TOF): m/z $[M]^+$ calcd for $C_{18}H_{13}FeI$ 411.9406; found 411.9387.

*1-(Iodoethynyl)-2-(naphthalen-2-yl)ferrocene (**11b**).* Conditions a: **11b** (73 mg, 63%) obtained from **6b** (0.25 mmol, 102 mg). Red solid. Mp: 114−116 °C. ^{1}H NMR (500 MHz, $CDCl_3$): δ 8.21 (s, 1H), 7.93 (d, J = 8.5 Hz, 1H), 7.84 (m, 3H), 7.47 (m, 2H), 4.73 (br s, 1H), 4.66 (br s, 1H), 4.38 (m, 1H), 4.16 (s, 5H). ^{13}C NMR (126 MHz, $CDCl_3$): δ 135.3, 133.5, 132.5, 128.0, 127.8, 127.6, 126.6, 126.3, 125.9, 125.8, 92.3, 88.1, 73.5, 71.7, 68.8, 68.7, 64.8, 2.3. Mp: 126−128 °C. HRMS (ESI-TOF): m/z $[M]^+$ calcd for $C_{22}H_{15}FeI$ 461.9562; found 461.9547.

*(S_{Fc})-1-(Iodoethynyl)-2-(naphthalene-2-yl)ferrocene ((S_{Fc})-**11b**).* Conditions a: (S_{Fc})-**11b** (137 mg, 67%) obtained from (S_{Fc})-**6b** (0.44 mmol, 180 mg). Red solid. Mp: 127−129 °C. $[\alpha]_D^{20}$ = +90 (c = 0.4, $CHCl_3$). HRMS (ESI-TOF): m/z $[M]^+$ calcd for $C_{22}H_{15}FeI$ 461.9562; found 461.9541.

*1-(Iodoethynyl)-3-phenylferrocene (**12a**).* Conditions a: **12a** (10 mg, 45%) obtained from **7a** (0.053 mmol, 19 mg). Red solid. Mp: 120−122 °C. ^{1}H NMR (500 MHz, $CDCl_3$): δ 7.42 (dd, J = 8.0, 1.5 Hz, 2H), 7.27 (t, J = 8.0 Hz, 2H), 7.19 (dt, J = 7.5, 1.5 Hz, 1H), 4.90 (t, J = 1.5 Hz, 1H), 4.64 (dd, J = 2.5, 1.5 Hz, 1H), 4.57 (dd, J = 2.5, 1.5 Hz, 1H), 4.09 (s, 5H). ^{13}C NMR (126 MHz, $CDCl_3$): δ 138.0, 128.6, 126.6, 126.3, 91.9, 86.3, 72.6, 71.7, 70.1, 67.2, 66.5, 0.0. HRMS (ESI-TOF): m/z $[M]^+$ calcd for $C_{18}H_{13}FeI$ 411.9406; found 411.9391.

*(S_{Fc})-1-(Iodoethynyl)-3-phenylferrocene ((S_{Fc})-**12a**).* Conditions a: (S_{Fc})-**12a** (65 mg, 56%) obtained from (S_{Fc})-**7a** (0.28 mmol, 100 mg). Red solid. Mp: 132−134 °C. $[\alpha]_D^{20}$ = +33 (c = 0.5, $CHCl_3$). HRMS (ESI-TOF): m/z $[M]^+$ calcd for $C_{18}H_{13}FeI$ 411.9406; found 411.9400.

*1-(Iodoethynyl)-3-(naphthalene-2-yl)ferrocene (**12b**).* Conditions a: **12b** (8 mg, 44%) obtained from **7b** (0.039 mmol, 16 mg). Red solid. Mp: 66−68 °C. ^{1}H NMR (500 MHz, $CDCl_3$): δ 7.84 (s, 1H), 7.79 (t, J = 8.0 Hz, 3H), 7.60 (dd, J = 8.5, 1.5 Hz, 1H), 7.46 (m, 2H), 5.05 (br s, 1H), 4.79 (m, 1H), 4.65 (m, 1H), 4.13 (s, 5H). ^{13}C NMR (126 MHz, $CDCl_3$): δ 135.6, 133.7, 132.4, 128.1, 127.9, 127.7, 126.5, 125.7, 125.1, 124.6, 91.9, 86.1, 72.9, 71.7, 70.2, 67.2, 66.8, 0.2. HRMS (ESI-TOF): m/z $[M]^+$ calcd for $C_{22}H_{15}FeI$ 461.9562; found 461.9554.

*(S_{Fc})-1-(Iodoethynyl)-3-(naphthalen-2-yl)ferrocene ((S_{Fc})-**12b**).* Conditions a: (S_{Fc})-**12b** (55 mg, 49%) obtained from (S_{Fc})-**7b** (0.28 mmol, 100 mg). Conditions d: (S_{Fc})-**12b** (14 mg, 62%) obtained from (S_{Fc})-**7b** (0.049 mmol, 20 mg). Red solid. Mp: 68−70 °C. $[\alpha]_D^{20}$ = +60 (c = 0.3, $CHCl_3$). HRMS (ESI-TOF): m/z $[M]^+$ calcd for $C_{22}H_{15}FeI$ 461.9562; found 461.9559.

*1-(Iodoethynyl)-2-methylferrocene (**13**).* Conditions a: **13** (47 mg, 50%) obtained from **8** (0.27 mmol, 80 mg). Red solid. Mp: 93−95 °C. ^{1}H NMR (500 MHz, $CDCl_3$): δ 4.35 (dd, J = 2.5, 1.5 Hz, 1H), 4.14 (m, 1H), 4.13 (s, 5H), 4.04 (t, J = 2.5 Hz, 1H), 2.09 (s, 3H). ^{13}C NMR (126 MHz, $CDCl_3$): δ 91.8, 87.2, 70.8, 70.7, 69.6, 67.0, 66.5, 13.8, 0.3. HRMS (ESI-TOF): m/z $[M]^+$ calcd for $C_{13}H_{11}FeI$ 349.9249; found 349.9236.

*(R_{Fc})-1-(Iodoethynyl)-2-methylferrocene ((R_{Fc})-**13**).* Conditions a: (R_{Fc})-**13** (46 mg, 39%) obtained from (R_{Fc})-**8** (0.338 mmol, 100 mg). Conditions d: (R_{Fc})-**13** (12 mg, 73%) obtained from (R_{Fc})-**8** (0.047 mmol, 14 mg). Red solid. Mp: 153−155 °C. $[\alpha]_D^{20}$ = −9 (c = 0.47, $CHCl_3$). HRMS (ESI-TOF): m/z $[M]^+$ calcd for $C_{13}H_{11}FeI$ 349.9249; found 349.9233.

General Procedure for the Alkyne Sulfanylation. The alkyne (1 equiv) was dissolved in THF (2 mL/mmol), and the solution was cooled to −78 °C. *n*-BuLi (1.6 M, 1 equiv) was added, and stirring was continued for 1 h. A solution of *N*-methyl-*N*-[(trifluoromethyl)-sulfanyl]aniline (1 equiv) in THF (0.5 mL/mmol) was added, and the mixture was stirred at −78 °C for 3 h. HCl (6 M) was added, and the mixture was extracted with pentane and the extract washed with HCl (6 M) and water and dried over Na_2SO_4. After filtration and concentration, the crude product was purified by chromatography on silica gel (pentane) to give the expected product.

*((2-Chloroferrocenyl)ethynyl)(trifluoromethyl)sulfane (**16a**).* Red oil (47 mg, 68%) obtained from **14** (0.2 mmol, 49 mg). ^{1}H NMR (500 MHz, $CDCl_3$): δ 4.56 (dd, J = 2.5, 1.5 Hz, 1H), 4.47 (dd, J = 2.5, 1.5 Hz, 1H), 4.29 (s, 5H), 4.20 (t, J = 2.5 Hz, 1H). ^{13}C NMR (126 MHz, $CDCl_3$): δ 127.8 (q, J = 313.7 Hz), 99.4, 95.5, 72.6, 70.6, 69.6, 67.2, 66.2 (d, J = 4.2 Hz), 62.6. ^{19}F NMR (75 MHz, $CDCl_3$): δ −44.4. HRMS (ESI-TOF): m/z $[M]^+$ calcd for $C_{13}H_8ClF_3FeS$ 343.9331; found 343.9352.

*((3-Chloroferrocenyl)ethynyl)(trifluoromethyl)sulfane (**16b**).* Red oil (22 mg, 52%) obtained from **15** (0.123 mmol, 30 mg). ^{1}H NMR (500 MHz, $CDCl_3$): δ 4.76 (br s, 1H), 4.52 (br s, 1H), 4.44 (br s, 1H), 4.31 (s, 5H). ^{13}C NMR (126 MHz, $CDCl_3$): δ 127.8 (q, J = 313.4 Hz), 101.0, 92.8, 72.5, 72.0, 71.0, 69.9, 63.6 (d, J = 4.3 Hz), 60.8. ^{19}F NMR (75 MHz, $CDCl_3$): δ −44.4. HRMS (ESI-TOF): m/z $[M]^+$ calcd for $C_{13}H_8ClF_3FeS$ 343.9331; found 343.9332.

General Procedure for the Alkyne Selenation. In one flask under argon were added benzyl(trifluoromethyl)selane (1 equiv) and THF (1 mL/mmol). Sulfuryl chloride (1 equiv) was added at room temperature, and the mixture was stirred for 15 min and then cooled to −78 °C. In a second flask, the alkyne (1.5 equiv) was dissolved in THF (2 mL/mmol) and the solution was cooled to −78 °C. *n*-BuLi (1.4 M in hexanes, 1.4 equiv) was added, and the mixture was stirred for 1 h. The alkynyllithium solution was cannulated to the first flask at −78 °C. After the mixture was stirred for 10 min, the temperature was raised to ambient temperature. Water was added, and the mixture was extracted with Et_2O and the extract dried over Na_2SO_4. After filtration and concentration, the crude product was purified by chromatography on silica gel (pentane) to give the expected product.

*((2-Chloroferrocenyl)ethynyl)(trifluoromethyl)selane (**17a**).* Red oil (104 mg, 71% based on benzyl(trifluoromethyl)selane) obtained from **14** (0.558 mmol, 136 mg), benzyl(trifluoromethyl)selane (0.372 mmol, 88 mg), and sulfuryl chloride (0.372 mmol, 30 μL). ^{1}H NMR (500 MHz, $CDCl_3$): δ 4.55 (br s, 1H), 4.46 (br s, 1H), 4.29 (s, 5H), 4.19 (t, J = 2.5 Hz, 1H). ^{13}C NMR (126 MHz, $CDCl_3$): δ 120.3 (q, J = 337.4 Hz), 104.7, 95.3, 72.5, 70.3, 69.3, 67.0, 63.3, 61.3 (d, J = 3.2 Hz). ^{19}F NMR (75 MHz, $CDCl_3$): δ −36.9. HRMS (ESI-TOF): m/z $[M]^+$ calcd for $C_{13}H_8ClF_3FeSe$ 391.8776; found 391.8793.

*((3-Chloroferrocenyl)ethynyl)(trifluoromethyl)selane (**17b**).* The general procedure was performed on **15** (0.131 mmol, 32 mg), benzyl(trifluoromethyl)selane (0.087 mmol, 21 mg), and sulfuryl chloride (0.087 mmol, 5.7 μL). After purification, the mixture (27 mg) was dissolved in DMSO (2 mL) and $LiOH{\cdot}H_2O$ (0.66 mmol, 28 mg) was added. After it was stirred for 4 h, the mixture was poured on ice and extracted with Et_2O. After drying over Na_2SO_4, filtration, and concentration, the crude product was purified by chromatography on silica gel (pentane) to give **17b** (15 mg, 44% based on benzyl-(trifluoromethyl)selane) as a red solid. Mp: 36−38 °C. ^{1}H NMR (500 MHz, $CDCl_3$): δ 4.75 (br s, 1H), 4.51 (br s, 1H), 4.43 (br s, 1H), 4.31 (s, 5H). ^{13}C NMR (126 MHz, $CDCl_3$): δ 120.3 (q, J = 337.3 Hz), 106.4, 92.7, 72.5, 71.8, 70.7, 69.7, 61.5, 61.3 (d, J = 5.0 Hz). ^{19}F NMR (75 MHz, $CDCl_3$): δ −36.9. HRMS (ESI-TOF): m/z $[M]^+$ calcd for $C_{13}H_8ClF_3FeSe$ 391.8776; found 391.8771.

https://dx.doi.org/10.1021/acs.organomet.0c00633
Organometallics XXXX, XXX, XXX−XXX

General Procedure for the Ritter Reaction. Benzhydryl bromide **32** (0.04 mmol, 9.9 mg) was placed in a flask under argon. A 2 mL portion of a stock solution (prepared by mixing 30 mL of CH_3CN and 14.4 μL of H_2O) was added, followed by a solution of iodoalkyne activator (0.04 mmol) in 1 mL of the same stock solution (note: iodoalkyne **11b** was not soluble in CH_3CN and was added as a solid). After it was stirred for 10 h at room temperature, the mixture was filtered on Celite and evaporated. The residue was analyzed by ^{1}H NMR in CD_3CN (see spectra in the Supporting Information).

General Procedure for Benzoxazole Synthesis. Thioacetamide **34** (0.2 mmol, 15 mg), 2-aminophenol (0.4 mmol, 43.6 mg), and the catalyst (0.02 mmol) were placed in a resealable tube under argon. Degassed toluene (0.4 mL) was added, and the mixture was stirred for 15 h at 90 °C. After it was cooled to room temperature, the crude product was filtered on Celite, washed with diethyl ether, and concentrated with a rotavap at 20 °C (the use of high vacuum must be avoided). A 1 mL portion of a 0.2 M solution of DMF in dichloromethane was added. Dichloromethane was removed with a rotavap at 20 °C, and the residue was analyzed by ^{1}H NMR (see spectra in the Supporting Information).

X-ray Structure Determination. X-ray crystallographic data were collected at low temperature on a CCD or CMOS diffractometer using Mo Kα radiation.

*Crystal Data for (S_{Fc})-**9a**:* $C_{12}H_8BrFeI$, M_r 414.84, monoclinic, a = 8.0567(7) Å, b = 9.2384(8) Å, c = 8.9782(7) Å, β = 115.956(3)°, V = 600.85(9) Å^3, T = 100(2) K, space group $P2_1$, Z = 2, μ(Mo Kα) = 7.111 mm^{-1}, 30382 reflections measured, 5746 independent reflections (R_{int} = 0.0394). Flack parameter = 0.007(9). The final R1 values were 0.0224 ($I > 2\sigma(I)$) and 0.0241 (all data). The final wR(F^2) values were 0.0533 ($I > 2\sigma(I)$) and 0.0540 (all data). The goodness of fit on F^2 was 1.041. CCDC no. 1995956.

*Crystal Data for (S_{Fc})-**9c**:* $C_{12}H_8FFeI$. M_r 353.93, orthorhombic, a = 16.4655(16) Å, b = 8.9985(8) Å, c = 7.3936(7) Å, V = 1095.47(18) Å^3, T = 100(2) K, space group $P2_12_12_1$, Z = 4, μ(Mo Kα) = 4.168 mm^{-1}, 32379 reflections measured, 5244 independent reflections (R_{int} = 0.0331). Flack parameter = 0.00(2). The final R1 values were 0.0176 ($I > 2\sigma(I)$) and 0.0184 (all data). The final wR(F^2) values were 0.0441 ($I > 2\sigma(I)$) and 0.0444 (all data). The goodness of fit on F^2 was 1.090. CCDC no. 1995957.

*Crystal Data for **9c**:* $C_{12}H_8FFeI$. M_r 353.93, orthorhombic, a = 16.43910(10) Å, b = 8.99930(10) Å, c = 7.41700(10) Å, V = 1097.27(2) Å^3, T = 100(2) K, space group *Pnma*, Z = 4, μ(Mo Kα) = 4.161 mm^{-1}, 79465 reflections measured, 2761 independent reflections (R_{int} = 0.0482). The final R1 values were 0.0183 ($I > 2\sigma(I)$) and 0.0198 (all data). The final wR(F^2) values were 0.0483 ($I > 2\sigma(I)$) and 0.0490 (all data). The goodness of fit on F^2 was 1.090. CCDC no. 1995952.

*Crystal Data for (S_{Fc})-**11a**:* $C_{18}H_{13}FeI$. M_r 412.03, orthorhombic, a = 8.8955(9) Å, b = 10.9653(11) Å, c = 15.3106(17) Å, V = 1493.4(3) Å^3, T = 100(2) K, space group $P2_12_12_1$, Z = 4, μ(Mo Kα) = 3.063 mm^{-1}, 190633 reflections measured, 8528 independent reflections (R_{int} = 0.0328). Flack parameter = −0.017(14). The final R1 values were 0.0208 (I > 2σ(I)) and 0.0245 (all data). The final wR(F^2) values were 0.0462 (I > 2σ(I)) and 0.0473 (all data). The goodness of fit on F^2 was 1.072. CCDC no. 1995958.

*Crystal Data for (S_{Fc})-**11b**:* $C_{22}H_{15}FeI$. M_r 462.09, orthorhombic, a = 8.4360(6) Å, b = 10.9150(7) Å, c = 19.1274(13) Å, V = 1761.2(2) Å^3, T = 100(2) K, space group $P2_12_12_1$, Z = 4, μ(Mo Kα) = 2.608 mm^{-1}, 28923 reflections measured, 8376 independent reflections (R_{int} = 0.0342). Flack parameter = −0.01(2). The final R1 values were 0.0381 ($I > 2\sigma(I)$) and 0.0609 (all data). The final wR(F^2) values were 0.0730 ($I > 2\sigma(I)$) and 0.0802 (all data). The goodness of fit on F^2 was 1.033. CCDC no. 1995959.

*Crystal Data for **11b**:* $C_{22}H_{15}FeI$. M_r 462.09, monoclinic, a = 8.1177(2) Å, b = 11.1905(2) Å, c = 18.9284(5) Å, β = 90.164(2) °, V = 1719.47(7) Å^3, T = 100(2) K, space group $P2_1/n$, Z = 4, μ(Mo Kα) = 2.671 mm^{-1}, 31600 reflections measured, 5160 independent reflections (R_{int} = 0.0445). The final R1 values were 0.0412 ($I > 2\sigma(I)$) and 0.0505 (all data). The final wR(F^2) values were 0.0887 ($I > 2\sigma(I)$) and 0.0925 (all data). The goodness of fit on F^2 was 1.064. CCDC no. 1995954.

*Crystal Data for (S_{Fc})-**12a**:* $C_{18}H_{13}FeI$. M_r 412.03, monoclinic, a = 9.7598(10) Å, b = 7.8063(8) Å, c = 10.0468(11) Å, β = 105.676(4) °, V = 736.97(13) Å^3, T = 100(2) K, space group $P2_1$, Z = 2, μ(Mo Kα) = 3.103 mm^{-1}, 43287 reflections measured, 7044 independent reflections (R_{int} = 0.0478). Flack parameter = −0.01(2). The final R1 values were 0.0330 ($I > 2\sigma(I)$) and 0.0461 (all data). The final wR(F^2) values were 0.0588 ($I > 2\sigma(I)$) and 0.0620 (all data). The goodness of fit on F^2 was 1.067. CCDC no. 1995960.

*Crystal Data for (R_{Fc})-**13**:* $C_{13}H_{11}FeI$. M_r 349.97, monoclinic, a = 8.1541(11) Å, b = 8.9666(12) Å, c = 9.0907(12) Å, β = 116.395(4) °, V = 595.37(14) Å^3, T = 100(2) K, space group $P2_1$, Z = 2, μ(Mo Kα) = 3.822 mm^{-1}, 61869 reflections measured, 5702 independent reflections (R_{int} = 0.0333). Flack parameter = 0.007(12). The final R1 values were 0.0118 ($I > 2\sigma(I)$) and 0.0121 (all data). The final wR(F^2) values were 0.0318 ($I > 2\sigma(I)$) and 0.0319 (all data). The goodness of fit on F^2 was 1.043. CCDC no. 1995953.

*Crystal Data for **13**:* $C_{13}H_{11}FeI$. M_r 349.97, monoclinic, a = 13.14030(10) Å, b = 12.99390(10) Å, c = 14.08200(10) Å, β = 103.6150(10) °, V = 2336.85(3) Å^3, T = 100(2) K, space group $P2_1/c$, Z = 8, μ(Mo Kα) = 3.895 mm^{-1}, 87060 reflections measured, 11589 independent reflections (R_{int} = 0.0341). The final R1 values were 0.0209 ($I > 2\sigma(I)$) and 0.0285 (all data). The final wR(F^2) values were 0.0471 ($I > 2\sigma(I)$) and 0.0493 (all data). The goodness of fit on F^2 was 1.046. CCDC no. 1995955.

■ ASSOCIATED CONTENT

Supporting Information

The Supporting Information is available free of charge at https://pubs.acs.org/doi/10.1021/acs.organomet.0c00633.

^{1}H and ^{13}C NMR spectra of all new compounds, HPLC and computational details, and XRD details for the structures of (S_{Fc})-**9a**, (S_{Fc})-**9c**, **9c**, (S_{Fc})-**11a**, (S_{Fc})-**11b**, **11b**, (S_{Fc})-**12a**, (R_{Fc})-**13**, and **13** (PDF)

Accession Codes

CCDC 1995952−1995960 contain the supplementary crystallographic data for this paper. These data can be obtained free of charge via www.ccdc.cam.ac.uk/data_request/cif, or by emailing data_request@ccdc.cam.ac.uk, or by contacting The Cambridge Crystallographic Data Centre, 12 Union Road, Cambridge CB2 1EZ, UK; fax: +44 1223 336033.

■ AUTHOR INFORMATION

Corresponding Authors

Victor Mamane − *Institut de Chimie de Strasbourg, UMR CNRS 7177, Equipe LASYROC, 67008 Strasbourg Cedex, France*; orcid.org/0000-0001-8996-7880; Email: vmamane@unistra.fr

Paola Peluso − *Istituto di Chimica Biomolecolare ICB, CNR, Sede secondaria di Sassari, 07100 Li Punti, Sassari, Italy*; Email: paola.peluso@cnr.it

Authors

Emmanuel Aubert − *Cristallographie, Résonance Magnétique et Modélisations (CRM2), UMR CNRS 7036, Université de Lorraine, 54506 Vandoeuvre-les-Nancy, France*

Robin Weiss − *Institut de Chimie de Strasbourg, UMR CNRS 7177, Equipe LASYROC, 67008 Strasbourg Cedex, France*

Emmanuel Wenger − *Cristallographie, Résonance Magnétique et Modélisations (CRM2), UMR CNRS 7036, Université de Lorraine, 54506 Vandoeuvre-les-Nancy, France*

Sergio Cossu − *Dipartimento di Scienze Molecolari e Nanosistemi DSMN, Università Ca' Foscari Venezia, 30172 Mestre Venezia, Italy*

https://dx.doi.org/10.1021/acs.organomet.0c00633
Organometallics XXXX, XXX, XXX−XXX

Patrick Pale − *Institut de Chimie de Strasbourg, UMR CNRS 7177, Equipe LASYROC, 67008 Strasbourg Cedex, France*

Complete contact information is available at: https://pubs.acs.org/10.1021/acs.organomet.0c00633

Notes

The authors declare no competing financial interest.

■ ACKNOWLEDGMENTS

This work was supported by the CNRS and University of Strasbourg. P.P. and S.C. are grateful to Università Ca' Foscari Venezia, Italy (Dipartimento di Scienze Molecolari e Nanosistemi, DSMN ADIR funds). We thank the PMD²X X-ray diffraction facility of the Institut Jean Barriol, Université de Lorraine, for X-ray diffraction measurements, data processing, and analysis and for providing reports for publication (http://crm2.univ-lorraine.fr/lab/fr/services/pmd2x). The EXPLOR mesocentre is thanked for providing access to their computing facility (project 2019CPMXX0984/wbg13). We thank J. N. Abergel for his help in the preparation of the starting dihaloferrocenes.

■ REFERENCES

(1) Politzer, P.; Murray, J. S.; Clark, T. Halogen Bonding and other σ-Hole Interactions: a Perspective. *Phys. Chem. Chem. Phys.* **2013**, *15*, 11178−11189.

(2) Cavallo, G.; Metrangolo, P.; Milani, R.; Pilati, T.; Priimagi, A.; Resnati, G.; Terraneo, G. The Halogen Bond. *Chem. Rev.* **2016**, *116*, 2478−2601.

(3) Tepper, R.; Schubert, U. S. Halogen Bonding in Solution: Anion Recognition, Templated Self-Assembly, and Organocatalysis. *Angew. Chem., Int. Ed.* **2018**, *57*, 6004−6016.

(4) Vogel, L.; Wonner, P.; Huber, S. M. Chalcogen Bonding: An Overview. *Angew. Chem., Int. Ed.* **2019**, *58*, 1880−1891.

(5) Scilabra, P.; Terraneo, G.; Resnati, G. The Chalcogen Bond in Crystalline Solids: A World Parallel to Halogen Bond. *Acc. Chem. Res.* **2019**, *52*, 1313−1324.

(6) Lim, J. Y. C.; Beer, P. D. Sigma-Hole Interactions in Anion Recognition. *Chem.* **2018**, *4*, 731−783.

(7) Sutar, R.; Huber, S. M. Catalysis of Organic Reactions through Halogen Bonding. *ACS Catal.* **2019**, *9*, 9622−9639.

(8) Bamberger, J.; Ostler, F.; et al. García Mancheño, O. Frontiers in Halogen and Chalcogen-Bond Donor Organocatalysis. *ChemCatChem* **2019**, *11*, 5198−5211.

(9) Peluso, P.; Mamane, V.; Aubert, E.; Cossu, S. Insights into the Impact of Shape and Electronic Properties on The Enantioseparation of Polyhalogenated 4,4′-Bipyridines on Polysaccharide-Type Selectors. Evidence of Stereoselective Halogen Bonding Interactions. *J. Chromatogr. A* **2014**, *1345*, 182−192.

(10) Peluso, P.; Mamane, V.; Aubert, E.; Dessi, A.; Dallocchio, R.; Dore, A.; Pale, P.; Cossu, S. Insights into Halogen Bond Driven Enantioseparations. *J. Chromatogr. A* **2016**, *1467*, 228−238.

(11) Peluso, P.; Mamane, V.; Dallocchio, R.; Dessi, A.; Villano, R.; Sanna, D.; Aubert, E.; Pale, P.; Cossu, S. Polysaccharide-Based Chiral Stationary Phases as Halogen Bond Acceptors: A Novel Strategy for Detection of Stereoselective σ-Hole Bonds in Solution. *J. Sep. Sci.* **2018**, *41*, 1247−1256.

(12) Dallocchio, R.; Dessi, A.; Solinas, M.; Arras, A.; Cossu, S.; Aubert, E.; Mamane, V.; Peluso, P. Halogen Bond in High-Performance Liquid Chromatography Enantioseparations: Description, Features and Modelling. *J. Chromatogr. A* **2018**, *1563*, 71−81.

(13) Peluso, P.; Gatti, C.; Dessi, A.; Dallocchio, R.; Weiss, R.; Aubert, E.; Pale, P.; Cossu, S.; Mamane, V. Enantioseparation of Fluorinated 3-Arylthio-4,4′-Bipyridines: Insights into Chalcogen and π-Hole Bonds in High-Performance Liquid Chromatography. *J. Chromatogr. A* **2018**, *1567*, 119−129.

(14) Peluso, P.; Mamane, V.; Dessì, A.; Dallocchio, R.; Aubert, E.; Gatti, C.; Mangelings, D.; Cossu, S. Halogen Bond in Separation Science: a Critical Analysis across Experimental and Theoretical Results. *J. Chromatogr. A* **2020**, *1616*, 460788.

(15) Lim, J. Y. C.; Marques, I.; Ferreira, L.; Félix, V.; Beer, P. D. Enhancing the Enantioselective Recognition and Sensing of Chiral Anions by Halogen Bonding. *Chem. Commun.* **2016**, *52*, 5527−5530.

(16) Borissov, A.; Lim, J. Y. C.; Brown, A.; Christensen, K. E.; Thompson, A. L.; Smith, M. D.; Beer, P. D. Neutral Iodotriazole Foldamers as Tetradentate Halogen Bonding Anion Receptors. *Chem. Commun.* **2017**, *53*, 2483−2486.

(17) Lim, J. Y. C.; Marques, I.; Félix, V.; Beer, P. D. Enantioselective Anion Recognition by Chiral Halogen-Bonding [2]Rotaxanes. *J. Am. Chem. Soc.* **2017**, *139*, 12228−12239.

(18) Lim, J. Y. C.; Marques, I.; Félix, V.; Beer, P. D. A Chiral Halogen-Bonding [3]Rotaxane for the Recognition and Sensing of Biologically Relevant Dicarboxylate Anions. *Angew. Chem., Int. Ed.* **2018**, *57*, 584−588.

(19) Kaasik, M.; Kaabel, S.; Kriis, K.; Järving, I.; Aav, R.; Rissanen, K.; Kanger, T. Synthesis and Characterisation of Chiral Triazole-Based Halogen-Bond Donors: Halogen Bonds in the Solid State and in Solution. *Chem. - Eur. J.* **2017**, *23*, 7337−7344.

(20) Peterson, A.; Kaasik, M.; Metsala, A.; Jarving, I.; Adamson, J.; Kanger, T. Tunable Chiral Triazole-Based Halogen Bond Donors: Assessment of Donor Strength in Solution with Nitrogen-Containing Acceptors. *RSC Adv.* **2019**, *9*, 11718−11721.

(21) Kuwano, S.; Suzuki, T.; Hosakaa, Y.; Arai, T. A Chiral Organic Base Catalyst with Halogen-Bonding-Donor Functionality: Asymmetric Mannich Reactions of Malononitrile with *N*-Boc Aldimines and Ketimines. *Chem. Commun.* **2018**, *54*, 3847−3850.

(22) Kuwano, S.; Nishida, Y.; Suzuki, T.; Arai, T. Catalytic Asymmetric Mannich-Type Reaction of Malononitrile with *N*-Boc α-Ketiminoesters Using Chiral Organic Base Catalyst with Halogen Bond Donor Functionality. *Adv. Synth. Catal.* **2020**, *362*, 1674−1678.

(23) Sutar, R. L.; Engelage, E.; Stoll, R.; Huber, S. M. Bidentate Chiral Bis(imidazolium)-Based Halogen-Bond Donors: Synthesis and Applications in Enantioselective Recognition and Catalysis. *Angew. Chem., Int. Ed.* **2020**, *59*, 6806−6810.

(24) Weiss, R.; Aubert, E.; Peluso, P.; Cossu, S.; Pale, P.; Mamane, V. Chiral Chalcogen Bond Donors Based on the 4,4′-Bipyridine Scaffold. *Molecules* **2019**, *24*, 4484.

(25) Goroff, N. S.; Curtis, S. M.; Webb, J. A.; Fowler, F. W.; Lauher, J. W. Designed Cocrystals Based on the Pyridine−Iodoalkyne Halogen Bond. *Org. Lett.* **2005**, *7*, 1891−1893.

(26) Gonzalez, L.; Gimeno, N.; Tejedor, R. M.; Polo, V.; Ros, M. B.; Uriel, S.; Serrano, J. L. Halogen-Bonding Complexes Based on Bis(iodoethynyl)benzene Units: A New Versatile Route to Supramolecular Materials. *Chem. Mater.* **2013**, *25*, 4503−4510.

(27) Aakeröy, C. B.; Wijethunga, T. K.; Desper, J.; Đakovic, M. Crystal Engineering with Iodoethynylnitrobenzenes: A Group of Highly Effective Halogen-Bond Donors. *Cryst. Growth Des.* **2015**, *15*, 3853−3861.

(28) Laurence, C.; Queignec-Cabanetos, M.; Dziembowska, T.; Queignec, R.; Wojtkowiak, B. 1-Iodoacetylenes. 1. Spectroscopic Evidence of Their Complexes with Lewis Bases. A Spectroscopic Scale of Soft Basicity. *J. Am. Chem. Soc.* **1981**, *103*, 2567−2573.

(29) Dumele, O.; Wu, D.; Trapp, N.; Goroff, N.; Diederich, F. Halogen Bonding of (Iodoethynyl)benzene Derivatives in Solution. *Org. Lett.* **2014**, *16*, 4722−4725.

(30) Matsuzawa, A.; Takeuchi, S.; Sugita, K. Iodoalkyne-Based Catalyst-Mediated Activation of Thioamides through Halogen Bonding. *Chem. - Asian J.* **2016**, *11*, 2863−2866.

(31) Perera, M. D.; Aakeröy, C. B. Organocatalysis by A Multidentate Halogen-Bond Donor: An Alternative to Hydrogen-Bond Based Catalysis. *New J. Chem.* **2019**, *43*, 8311−8314.

(32) Sharma, P.; Singh, R. R.; Giri, S. S.; Chen, L.-Y.; Cheng, M.-J.; Liu, R.-S. Gold-Catalyzed Oxidation of Thioalkynes to Form Phenylthio Ketene Derivatives via a Noncarbene Route. *Org. Lett.* **2019**, *21*, 5475−5479.

(33) Song, W.; Zheng, N.; Li, M.; He, J.; Li, J.; Dong, K.; Ullah, K.; Zheng, Y. Rhodium(I)-Catalyzed Regioselective Azide-internal Alkynyl Trifluoromethyl Sulfide Cycloaddition and Azide-internal Thioalkyne Cycloaddition under Mild Conditions. *Adv. Synth. Catal.* **2019**, *361*, 469−475.
(34) Coelho, F. L.; Gil, E. S.; Gonçalves, P. F. B.; Campo, L. F.; Schneider, P. H. Intramolecular Hydroamination of Selenoalkynes to 2-Selenylindoles in the Absence of Catalyst. *Chem. - Eur. J.* **2019**, *25*, 8157−8162.
(35) Baldassari, L. L.; Mantovani, A. C.; Senoner, S.; Maryasin, B.; Maulide, N.; Lüdtke, D. S. Redox-Neutral Synthesis of Selenoesters by Oxyarylation of Selenoalkynes under Mild Conditions. *Org. Lett.* **2018**, *20*, 5881−5885.
(36) Schaarschmidt, D.; Lang, H. Selective Syntheses of Planar-Chiral Ferrocenes. *Organometallics* **2013**, *32*, 5668−5704.
(37) Dai, L.-X.; Tu, T.; You, S.-L.; Deng, W.-P.; Hou, X.-L. Asymmetric Catalysis with Chiral Ferrocene Ligands. *Acc. Chem. Res.* **2003**, *36*, 659−667.
(38) Mamane, V. Metal-Catalyzed Cross-Coupling Reactions for Ferrocene Functionalization: Recent Applications in Synthesis, Material Science and Asymmetric Catalysis. *Mini-Rev. Org. Chem.* **2008**, *5*, 303−312.
(39) Kuklin, S. A.; Sheloumov, A. M.; Dolgushin, F. M.; Ezernitskaya, M. G.; Peregudov, A. S.; Petrovskii, P. V.; Koridze, A. A. Highly Active Iridium Catalysts for Alkane Dehydrogenation. Synthesis and Properties of Iridium Bis(phosphine) Pincer Complexes Based on Ferrocene and Ruthenocene. *Organometallics* **2006**, *25*, 5466−5476.
(40) Ferber, B.; Top, S.; Vessières, A.; Welter, R.; Jaouen, G. Synthesis of Optically Pure *o*-Formylcyclopentadienyl Metal Complexes of 17α-Ethynylestradiol. Recognition of the Planar Chirality by the Estrogen Receptor. *Organometallics* **2006**, *25*, 5730−5739.
(41) Westwood, J.; Coles, S. J.; Collinson, S. R.; Gasser, G.; Green, S. J.; Hursthouse, M. B.; Light, M. E.; Tucker, J. H. R. Binding and Electrochemical Recognition of Barbiturate and Urea Derivatives by a Regioisomeric Series of Hydrogen-Bonding Ferrocene Receptors. *Organometallics* **2004**, *23*, 946−951.
(42) Lim, J. Y. C.; Beer, P. D. A Halogen Bonding 1,3-Disubstituted Ferrocene Receptor for Recognition and Redox Sensing of Azide. *Eur. J. Inorg. Chem.* **2017**, *2017*, 220−224.
(43) Walter, S. M.; Kniep, F.; Herdtweck, E.; Huber, S. M. Halogen-Bond-Induced Activation of a Carbon−Heteroatom Bond. *Angew. Chem., Int. Ed.* **2011**, *50*, 7187−7191.
(44) Aakeröy, C. B.; Baldrighi, M.; Desper, J.; Metrangolo, P.; Resnati, G. Supramolecular Hierarchy among Halogen-Bond Donors. *Chem. - Eur. J.* **2013**, *19*, 16240−16247.
(45) Torubaev, Y. V.; Skabitskya, I. V. The Energy Frameworks of aufbau Synthon Modules in 4-Cyanopyridine Co-crystals. *CrystEngComm* **2019**, *21*, 7057−7068.
(46) Torubaev, Y. V.; Skabitsky, I. V. The energy frameworks of aufbau synthon modules in 4-cyanopyridine co-crystals. *CrystEngComm* **2019**, *21*, 7057−7068.
(47) Dayaker, G.; Sreeshailam, A.; Chevallier, F.; Roisnel, T.; Krishna, P. R.; Mongin, F. Deprotonative Metallation of Ferrocenes using Mixed Lithium−Zinc and Lithium−Cadmium Combinations. *Chem. Commun.* **2010**, *46*, 2862−2864.
(48) Tazi, M.; Hedidi, M.; Erb, W.; Halauko, Y. S.; Ivashkevich, O. A.; Matulis, V. E.; Roisnel, T.; Dorcet, V.; Bentabed-Ababsa, G.; Mongin, F. Fluoro- and Chloroferrocene: From 2- to 3-Substituted Derivatives. *Organometallics* **2018**, *37*, 2207−2211.
(49) Tazi, M.; Erb, W.; Roisnel, T.; Dorcet, V.; Mongin, F.; Low, P. J. From Ferrocene to fluorine-Containing Pentasubstituted Derivatives and all Points in-between; or, how to Increase the Available Chemical Space. *Org. Biomol. Chem.* **2019**, *17*, 9352−9359.
(50) Chinchilla, R.; Najera, C. The Sonogashira Reaction: A Booming Methodology in Synthetic Organic Chemistry. *Chem. Rev.* **2007**, *107*, 874−922.
(51) Inkpen, M. S.; White, A. J. P.; Albrecht, T.; Long, N. J. Rapid Sonogashira Cross-Coupling of Iodoferrocenes and the Unexpected Cyclo-Oligomerization of 4-Ethynylphenylthioacetate. *Chem. Commun.* **2013**, *49*, 5663−5665.
(52) Wolfe, J. P.; Singer, R. A.; Yang, B. H.; Buchwald, S. L. Highly Active Palladium Catalysts for Suzuki Coupling Reactions. *J. Am. Chem. Soc.* **1999**, *121*, 9550−9561.
(53) Nishikawa, T.; Shibuya, S.; Hosokawa, S.; Isobe, M. One Pot Synthesis of Haloacetylenes from Trimethylsilylacetylenes. *Synlett* **1994**, *1994*, 485−486.
(54) Carty, P.; Dove, M. F. A. The Reaction of Some Ferrocenyl Ketones with Anhydrous Silver Tetrafluoroborate, a New Route to Substituted Ferricenium Salts. *J. Organomet. Chem.* **1971**, *28*, 125−132.
(55) Aguado, J. E.; Cativiela, C.; Gimeno, M. C.; Jones, P. G.; Laguna, A.; Sarroca, C. Unexpected Formation of Ferrocene-Containing Indolizines by Tandem Cyclization−Activation Reactions Induced by Silver Salts. *Eur. J. Inorg. Chem.* **2009**, *2009*, 216−219.
(56) Russo, M. V.; Sterzo, L.; Franceschini, P.; Biagini, G.; Furlani, A. Synthesis of Highly Ethynylated Mono and Dinuclear Pt(II) Tethers Bearing the 4,4′-Bis(Ethynyl)Biphenyl (debp) Unit as Central Core. *J. Organomet. Chem.* **2001**, *619*, 49−61.
(57) Baert, F.; Colomb, J.; Billard, T. Electrophilic Trifluoromethanesulfanylation of Organometallic Species with Trifluoromethanesulfanamides. *Angew. Chem., Int. Ed.* **2012**, *51*, 10382−10385.
(58) Glenadel, Q.; Ismalaj, E.; Billard, T. Electrophilic Trifluoromethyl- and Fluoroalkylselenolation of Organometallic Reagents. *Eur. J. Org. Chem.* **2017**, *2017*, 530−533.
(59) Glenadel, Q.; Ismalaj, E.; Billard, T. A Metal-Free Route to Heterocyclic Trifluoromethyl- and Fluoroalkylselenolated Molecules. *Org. Lett.* **2018**, *20*, 56−59.
(60) Zhong, L.; Savoie, P. R.; Filatov, A. S.; Welch, J. T. Preparation and Characterization of Alkenyl Aryl Tetrafluoro-l6-sulfanes. *Angew. Chem., Int. Ed.* **2014**, *53*, 526−529.
(61) Jiang, D.; He, T.; Ma, L.; Wang, Z. Recent Developments in Ritter Reaction. *RSC Adv.* **2014**, *4*, 64936−64946.
(62) Jagodzinski, T. Thioamides as Useful Synthons in the Synthesis of Heterocycles. *Chem. Rev.* **2003**, *103*, 197−228.
(63) Ritter, J. J.; Minieri, P. P. A New Reaction of Nitriles. I. Amides from Alkenes and Mononitriles. *J. Am. Chem. Soc.* **1948**, *70*, 4045−4048.
(64) For a review, see: Guérinot, A.; Reymond, S.; Cossy, J. Ritter Reaction: Recent Catalytic Developments. *Eur. J. Org. Chem.* **2012**, *2012*, 19−28.
(65) Kniep, F.; Rout, L.; Walter, S. M.; Bensch, H. K. V.; Jungbauer, S. H.; Herdtweck, E.; Huber, S. M. 5-Iodo-1,2,3-triazolium-Based Multidentate Halogen-Bond Donors as Activating Reagents. *Chem. Commun.* **2012**, *48*, 9299−9301.
(66) Kniep, F.; Walter, S. M.; Herdtweck, E.; Huber, S. M. 4,4′-Azobis(halopyridinium) Derivatives: Strong Multidentate Halogen-Bond Donors with a Redox-Active Core. *Chem. - Eur. J.* **2012**, *18*, 1306−1310.
(67) For a review, see: Gao, X.; Liu, J.; Zuo, X.; Feng, X.; Gao, Y. Recent Advances in Synthesis of Benzothiazole Compounds Related to Green Chemistry. *Molecules* **2020**, *25*, 1675.
(68) Zirakzadeh, A.; Groß, M. A.; Wang, Y.; Mereiter, K.; Spindler, F.; Weissensteiner, W. Biferrocene-Based Diphosphine Ligands: Synthesis and Application of Walphos Analogues in Asymmetric Hydrogenations. *Organometallics* **2013**, *32*, 1075−1084.
(69) Urbano, A.; del Hoyo, A. M.; Martínez-Carrion, A.; Carreño, M. C. Asymmetric Synthesis and Chiroptical Properties of Enantiopure Helical Ferrocenes. *Org. Lett.* **2019**, *21*, 4623−4627.
(70) Mamane, V. The Diastereoselective *ortho*-Lithiation of Kagan's Ferrocenyl Acetal. Generation and Reactivity of Chiral 2-Substituted Ferrocenecarboxaldehydes. *Tetrahedron: Asymmetry* **2010**, *21*, 1019−1029.
(71) Riant, O.; Samuel, O.; Flessner, T.; Taudien, S.; Kagan, H. B. An Efficient Asymmetric Synthesis of 2-Substituted Ferrocenecarboxaldehydes. *J. Org. Chem.* **1997**, *62*, 6733−6745.

https://dx.doi.org/10.1021/acs.organomet.0c00633
Organometallics XXXX, XXX, XXX−XXX

(72) Dhameja, M.; Pandey, J. Bestmann-Ohira Reagent: A Convenient and Promising Reagent in the Chemical World. *Asian J. Org. Chem.* **2018**, *7*, 1502−1523.
(73) Ferber, B.; Top, S.; Welter, R.; Jaouen, G. A New Efficient Route to Chiral 1,3-Disubstituted Ferrocenes: Application to the Syntheses of (*R*p)- and (*S*p)-17α-[(3′-formylferrocenyl)ethynyl]-estradiol. *Chem. - Eur. J.* **2006**, *12*, 2081−2086.
(74) Jelsch, C.; Ejsmont, K.; Huder, L. The Enrichment Ratio of Atomic Contacts in Crystals, an Indicator Derived from the Hirshfeld Surface Analysis. *IUCrJ* **2014**, *1*, 119−128.
(75) Torubaev, Y. V.; Lyssenko, K. A.; Barzilovich, P. Y.; Saratov, G. A.; Shaikh, M. M.; Singh, A.; Mathur, P. Self-Assembly of Conducting Cocrystals *via* Iodine···π(Cp) Interactions. *CrystEngComm* **2017**, *19*, 5114−5121.
(76) Baldrighi, M.; Bartesaghi, D.; Cavallo, G.; Chierotti, M. R.; Gobetto, R.; Metrangolo, P.; Pilati, T.; Resnati, G.; Terraneo, G. Polymorphs and Co-Crystals of Haloprogin: An Antifungal Agent. *CrystEngComm* **2014**, *16*, 5897−5904.
(77) Keith, T. A. *AIMAll (Version 19.10.12)*; TK Gristmill Software: Overland Park KS, USA, 2019 (aim.tkgristmill.com).
(78) Lu, T.; Chen, F. Multiwfn: A Multifunctional Wavefunction Analyzer. *J. Comput. Chem.* **2012**, *33*, 580−592.
(79) Lu, T.; Chen, F. Quantitative analysis of molecular surface based on improved Marching Tetrahedra algorithm. *J. Mol. Graphics Modell.* **2012**, *38*, 314−323.

https://dx.doi.org/10.1021/acs.organomet.0c00633
Organometallics XXXX, XXX, XXX−XXX